A Real-Time Proactive Intersection Safety Monitoring System Based on Video Data

FINAL REPORT
April 2022

Submitted by:
Mohammad Jalayer, Ph.D.
Associate Professor

Deep Patel
Research Assistant

Parisa Hosseini
Research Assistant

Nidhal Carla Bouaynaya, Ph.D.
Professor & Associate Dean for Research and Graduate Studies

Department of Civil and Environmental Engineering
Department of Electrical and Computer Engineering
Rowan University,
Glassboro, NJ, 08028

External Project Manager
Joseph Weiss, Transportation Safety Analyst
New Jersey Division of Highway Traffic Safety

In cooperation with
Rutgers, The State University of New Jersey
and
New Jersey Division of Highway Traffic Safety
and
U.S. Department of Transportation
Federal Highway Administration

Disclaimer Statement

The contents of this report reflect the views of the authors, who are responsible for the facts and the accuracy of the information presented herein. This document is disseminated. under the sponsorship of the Department of Transportation, University Transportation Centers Program, in the interest of information exchange. The U.S. Government assumes no liability for the contents or use thereof.

The Center for Advanced Infrastructure and Transportation (CAIT) is a Regional UTC Consortium led by Rutgers, The State University. Members of the consortium are Atlantic Cape Community College, Columbia University, Cornell University, New Jersey Institute of Technology, Polytechnic University of Puerto Rico, Princeton University, Rowan University, SUNY - Farmingdale State College, and SUNY - University at Buffalo. The Center is funded by the U.S. Department of Transportation.

1. Report No. CAIT-UTC-REG53	2. Government Accession No.	3. Recipient's Catalog No.	
4. Title and Subtitle A Real-Time Proactive Intersection Safety Monitoring System Based on Video Data		5. Report Date April 2022	
		6. Performing Organization Code CAIT/Rowan University	
7. Author(s) Mohammad Jalayer (https://orcid.org/0000-0001-6059-3942) Nidhal Carla Bouaynaya (https://orcid.org/0000-0002-8833-8414) Deep Patel (https://orcid.org/0000-0001-7595-7489) Parisa Hosseini (https://orcid.org/0000-0003-3488-3895)		8. Performing Organization Report No. CAIT-UTC-REG53	
9. Performing Organization Name and Address Department of Civil and Environmental Engineering Department of Electrical and Computer Engineering Rowan University, Glassboro, NJ, 08028		10. Work Unit No.	
		11. Contract or Grant No. 69A3551847102	
12. Sponsoring Agency Name and Address Center for Advanced Infrastructure and Transportation Rutgers, The State University of New Jersey 100 Brett Road Piscataway, NJ 08854		13. Type of Report and Period Covered Final Report 03/31/2021 - 02/28/2022	
		14. Sponsoring Agency Code	
15. Supplementary Notes U.S. Department of Transportation/OST-R; 1200 New Jersey Avenue, SE; Washington, DC 20590-0001			

16. **Abstract:** In recent years, identifying road users' behavior and conflicts at intersections have become an essential data source for evaluating traffic safety. According to the Federal Highway Administration (FHWA), in 2020, more than 50% of fatal and injury crashes occurred at or near the intersections, necessitating further investigation. This study developed an innovative artificial intelligence (AI)-based video analytic tool to assess intersection safety using surrogate safety measures. Surrogate safety measures (e.g., Post-encroachment Time (PET) and Time-to-Collision (TTC)) are extensively used to identify future threats, such as rear-end and left-turning collisions due to vehicle and road users' interactions. To extract the trajectory data, this project integrates a real-time AI detection model - YOLO-v5 with a tracking framework based on the DeepSORT algorithm. 54 hours of high-resolution video data were collected at six signalized intersections (including three 3-leg intersections and three 4-leg intersections) in Glassboro, New Jersey. Non-compliance behaviors, such as red-light running and pedestrian jaywalking, are captured to better understand the risky behaviors at these locations. The proposed approach achieved an accuracy of 92% to 98% for detecting and tracking the road users' trajectories. Additionally, a user-friendly web-based application was developed that provides directional traffic volumes, pedestrian volumes, vehicles running a red light, pedestrian jaywalking events, and PET and TTC for crossing conflicts between two road users. In addition, an extreme value theory (EVT) was used to estimate the number of crashes at each intersection utilizing the frequency of PETs and TTCs. Finally, the intersections were ranked based on the calculated score considering the severity of crashes. Overall, the developed tool as well as the crash estimation model and ranking method, can provide valuable information for engineers and policymakers to assess the safety of intersections and implement effective countermeasures to mitigate the intersection-involved crashes.

17. Key Words Intersection safety, surrogate safety measures, PET, TTC	18. Distribution Statement		
19. Security Classification (of this report) **Unclassified**	20. Security Classification (of this page) **Unclassified**	21. No. of Pages 44	22. Price

Table of Contents

List of Figures

List of Tables

EXECUTIVE SUMMARY

In recent years, identifying road users' behavior and conflicts at intersections have become an essential data source for evaluating traffic safety. According to the Federal Highway Administration (FHWA), in 2020, more than 50% of fatal and injury crashes occurred at or near intersections (FHWA, 2021). For the state of New Jersey, 146 fatal crashes occurred at intersections in 2019, indicating a 39% increase compared to the 105 fatal crashes that happened in 2015 (NJDSP, 2019). In addition, millions of minor crashes and conflicts are not reported every year due to their lower level of intensity. This increase in the crash fatality rate and unidentified traffic conflicts have raised concerns for the safety of road users at the intersection. Hence, there is a need to investigate the safety of road users at intersections.

This study developed an innovative artificial intelligence (AI)-based video analytic tool to assess intersection safety using surrogate safety measures. Surrogate safety measures (e.g., Post-encroachment Time (PET) and Time-to-Collision (TTC)) are extensively used to identify future threats, such as rear-end and left-turning collisions due to vehicle and road users' interactions. To extract the trajectory data, this project integrates a real-time AI detection model - YOLO-v5 with a tracking framework based on the DeepSORT algorithm. 54 hours of high-resolution video data were collected from six signalized intersections in Glassboro, New Jersey. Non-compliance behaviors, such as redlight running and pedestrian jaywalking, are captured to better understand the risky behaviors at the selected intersections. The proposed approach achieved an accuracy of between 92% to 99% for detecting and tracking the road users' trajectories. Additionally, a user-friendly web-based application provides direction-based vehicle volume, vehicles running a red light, PET, and TTC for vehicle-to-vehicle and vehicle-to-pedestrian, pedestrian volume, and pedestrian jaywalking events.

As the next step, extreme value theory (EVT) models with block maxima approach were developed, and the yearly crash frequencies for the 4-leg intersections were estimated by using the models' parameters estimates. Traffic conflict indicators, including PET and TTC, were implemented for developing the EVT models. Thereafter, by using the New Jersey left-turn crash severity distribution ratios, different severity levels of the estimated crashes were calculated. Finally, the crash severities were converted to Equivalent Property Damage Only (EPDO), and by combining the EPDOs estimated from both PET and TTC, the three 4-leg intersections were ranked based on their safety.

Overall, this project can provide transportation practitioners and policymakers with an automated AI-based video analytic tool to extract traffic conflict from video data. This study can also help transportation practitioners and policymakers with assessing the safety of intersections through a crash prediction and ranking approach in order to implement effective countermeasures for enhancing the safety of intersections.

CHAPTER 1. INTRODUCTION AND RESEARCH OBJECTIVES

In 2019, a total of 36,096 traffic fatalities occurred in the United States, according to the Federal Highway Administration (FHWA) (2022). Approximately 10,180 of the total fatalities involved intersections suggesting a 1.6% increase compared to the fatalities occurred in 2018. The great number of traffic fatalities and their increase in recent years has become a major concern for transportation agencies, necessitating the importance of studying the safety of road users at intersections. Developing safety assessment analysis usually needs a sufficient number of crash data. However, there are some limitations in preparing crash data, including the difficulties in the collection process, the long time needed for data collection, and under-reporting issues (Yang et al., 2021). Surrogate Safety Measures (SSMs) have gained a great deal of attention as an alternative approach for road safety analysis in recent years (Tarko et al., 2009; Zheng et al., 2014a; Laureshyn et al., 2017; Essa and Sayed, 2018). SSMs are also known as near-crash indicators, which measure and capture the temporal and spatial proximity of road users. Traffic conflict is one of the proactive SSM tools that can be implemented for road safety analysis. A traffic conflict is referred to "an observable situation in which two or more road users approach each other in space and time to such an extent that there is a risk of collision if their movements remain unchanged" (Amundsen and Hydén, 1977). There is a variety of traffic conflict indicators being used for measuring interaction safety. Post Encroachment Time (PET) and Time to Collision (TTC) are two of the most commonly used traffic conflicts being applied for safety analysis.

High-definition trajectory data is critical for identifying traffic conflicts, where several computer vision algorithms have been implemented to recognize and track road users from video data. (Simmonet et al., 2012; Manh and Alahband, 2018; Wang et al., 2019; Cai et al., 2019; Zhang et al., 2020). Recently, public authorities, vehicle manufacturers, and numerous scholars have been fascinated by computer vision techniques and have used video data for evaluating traffic safety (Sayed et al., 2013; Chen et al., 2017; Formosa et al., 2020; Zhang et al., 2020; Mahmoud et al., 2021). As part of this study, a real-time AI detection model - YOLO-v5, with a tracking framework based on the DeepSORT algorithm, was implemented to extract the trajectory data.

Once the trajectories data is extracted and traffic conflicts are identified, they can be further analyzed by implementing different statistical methods to develop a safety assessment of a specific road facility. In recent decades, several studies have been conducted in order to validate the applicability of traffic conflicts as an alternative method for road safety analysis. The validity of traffic conflicts is usually conducted by developing the correlation between traffic conflicts and crash frequency (Zheng et al., 2014b). One of the most often applied methods for evaluating validity is regression analysis (Hauerand Garder, 1986; Lord, 1996; Sayed and Zein, 1999; Lord and Mannering, 2010; EI-Basyouny and Sayed, 2013). However, due to the limitations of regression models, more sophisticated approaches, which are non-crash-based methods, have gained more attention in recent years. Extreme value theory (EVT) approach is one of the recent methods capable of estimating the possibility of extreme events from observations that occurred within a relatively short period.

The EVT has been extensively implemented as a powerful tool in many research areas to assess the distributions of extreme events. The areas of EVT applications include but are not limited to

hydrology for flood and draughts prediction (Fernandes et al., 2010), ocean engineering for wave height prediction (Jonathan and Ewans, 2013), finance for financial crisis prediction (Rocco, 2011), and meteorology for extreme wind prediction (Torrielli et al., 2013). EVT models are newly being employed in Transportation Engineering for road safety analysis. Initially, there were some limitations in applying EVT models in road safety analysis; however, these models have been gaining considerable attention in recent years. EVT models are being proposed in different approaches by using either one traffic conflict as a univariate model (Zheng et al., 2014a, 2019b; Zheng and Sayed, 2019b) or more than one traffic conflict as a bivariate/multivariate model (Wang et al., 2019; Zheng et al., 2018, 2019a; Zheng and Sayed, 2019a, 2020).

Research Objectives:

This project mainly focused on assessing the safety of road users at intersections. The main objectives of this project can be summarized as follows:

- To investigate the safety of intersections by using traffic conflict and non-compliance data
- To develop an automated AI-based video analytic tool to extract events including direction-based vehicle volume, vehicles running a red light, traffic conflicts (e.g., PET, and TTC) for both vehicle-to-vehicle and vehicle-to-pedestrian, pedestrian volume, and pedestrian jaywalking from video data
- To develop models for predicting the number of crashes at intersections by using traffic conflict indicators
- To develop a ranking method to rank the intersections based on their safety

CHAPTER 2. LITERATURE REVIEW

Examining intersection safety using SSMs has been implemented in many studies over recent years. A summary of previous studies that applied SSMs for safety evaluations at intersections is provided as follows:

In 2010, Saunier et al. (2010) investigated the road users interactions by developing a probabilistic framework. In order to predict the collision probabilities, possible collision points were identified, and their spatial distribution was plotted. The interactions in this study were divided into four groups, including rear-end, side, parallel, and head-on. Video data from Kentucky were collected having a record of around 300 collisions and severe interactions. This study proved that the proposed framework can be usefully applied for assessing road user behavior leading to collisions. In another study, Alhajyaseen (2015) developed a crash hazard measurement taking into account the crash severity and occurrence probability for investigating the safety of intersections. The author collected video data at signalized intersections for extracting the vehicle trajectories to estimate the conflict characteristics. In this study, they employed PET, angle of collision, and total kinetic energy change before and after the collision to develop the conflict index. The results indicated that the proposed safety measure is capable of successfully ranking the various signalized intersections based on the severity of the crashes. A year later, Zangenehpour et al. (2016) conducted a case-control study to assess the safety impacts of cycle track at intersections using ordered logit models. To do so, the authors developed a video-based approach in which the PET between the turning vehicles and cyclists both traveling in the same direction was considered as surrogate measures. They collected 90 hours of video data from 23 intersections in Montreal. Results indicated that intersections having cycle tracks on the right side are safer when compared to the intersections having no cycle tracks. It was also shown that the probability of a cyclist being involved in perilous interactions decreased with the increase in the size of the cyclist group reaching the intersection. In another study carried out by Xie et al. (2016), safety improvements were assessed by using traffic conflicts obtained from a traffic video recording. TTC for each vehicle pair was computed, and afterward, traffic control risks were determined. In this study, automatic video data collection and computer vision techniques in two intersections for 70 hours in Brooklyn, New York, were conducted. A robust correlation between traffic conflicts and actual crashes was observed. Therefore, they confirmed the validation of the mentioned method. In 2017, Cheng et al. (2017) investigated the applicability of using the Unmanned Aerial Vehicle (UAV) video for developing the surrogate safety analysis of pedestrian-to-vehicle conflicts at an urban intersection located in Beijing, China. As part of this study, 60 minutes of aerial video data were collected, and two SSMs, including relative time to collision (RTTC) and PET, were considered for further analysis. Results obtained from this study showed fairly risky behavior of right-turn vehicles around the corner. Results also showed high exposure of pedestrians to traffic conflict outside and inside of the crosswalk. Finally, the results of this study proved the capability of UAV in assessing the safety of an intersection in an accurate and cost-effective way. Devloping a framework to automatically mine massive vehicle trajectory data from video recordings using computer vision techniques is the main focus of a study conducted by Xie et al. (2019). To do so, 70 hours of video data were collected from two intersections located in New York City. TTC was considered as the surrogate safety measure for rear-end conflict identification. Afterward, five-minute interval rear-end conflicts were modeled using Hidden Markov models (HMMs). Finally, HMMs were employed to determine the hidden states of traffic safety. Results revealed that the HMMs having four hidden states and zero covariates for Jay & Johnson as well as the HMMs

having three hidden states and two covariates for Jay & Fulton perform the best in showing the conflict occurrence. Scholl et al. (2019) implemented an automated video analytics tool to assess surrogate traffic safety measures and the effectiveness of inexpensive countermeasures at selected pedestrian crossings at unsafe intersections. The authors utilized a computer vision software named BriskLUMINA to process video and generate data on trajectories and speed of the road users. The results showed that the key issues associated with pedestrian crash risk are motorcycles, turning movements, and roundabouts. The results also revealed that the applied treatments were efficient at 4-legged intersections. Yang et al. (2021) introduced a new safety performance measure named Risk Status (RS) by combining SSMs and crash data. Within the Safety Pilot Model Deployment (SPMD) project in Michigan, the SSMs were extracted using connected vehicle data. The relationship between the crash frequency, RS, contributing factors, and risk determined by SSMs was modeled by employing an equation with corridor-level random parameters and conditional autoregressive spatial effect. This study showed that the RS is a reliable criterion for investigating the safety in which the hotspot locations need to be identified. Also, the results indicated that the proposed RS at the same time could fuse SSMs and crash frequency and control for unobserved and observed heterogeneity. In one of the most recent studies, Nadimi et al. (2021) developed a performance comparison by statistically analyzing SSMs. To achieve this goal, the authors initially determine the eligible indicators. Then, they combine the eligible indicators by applying collision probability (CP), which is a recently used safety indicator. In this study, microscopic traffic data (obtained from the Next Generation Simulation (NGSIM) website) for Interstate 80 was collected and used for further analysis. Finally, the results were compared using the Pearson correlation coefficient and t-test. This study revealed that the proposed methodology could be a helpful framework for screening SSMs and determining the rear-end collision probability by considering merged SSMs.

In recent years, EVT has gained a great deal of attention for developing safety evaluations in the transportation engineering field. Many studies were carried out to investigate the safety intersections by implementing different traffic conflict indicators. In 2018, Wang et al. (2018) conducted a research that mainly focused on developing a safety evaluation by employing EVT. The authors collected the data for ten urban intersections located in Shanghai. In this study, in order to conduct the simulation analysis, three calibration strategies were utilized, including base strategy, semi-calibration strategy, and full-calibration strategy. Then, the simulated conflict data was obtained from vehicle trajectories generated in VISSIM by using the surrogate safety assessment model (SSAM). Field conflict data was also collected by trained observers. Finally, the field and simulated conflict data were modeled, and the Estimated Annual Crash Frequency (EACF) was determined by applying the EVT methodology with PET. The estimated EACFs derived from the three strategies were then compared with other conventional methods. Results indicated that the determining EACF using the full-calibration strategy works better for safety evaluations based on simulations. In an attempt to estimate the crash frequency, Zheng et al. (2019a) developed a bivariate extreme value model using different combinations of traffic conflicts. In this study, the authors utilized PET, TTC, MTTC, and DRAC as traffic conflicts. Theyrecorded 7 hours of video data from four intersections located in British Columbia, Canada. Then, they used computer vision techniques to determine the considered traffic conflicts from the recorded videos. The results from this study revealed that the combination of TTC&PET had the best performance in terms of accuracy in estimating crash frequencies. In a similar study, Zheng and Sayed (2019a) developed two different bivariate extreme value models, including Bivariate Generalized Extreme Value (BGEV) and Bivariate Generalized Pareto (BGP), in order to integrate

traffic conflicts for left-turn crash estimations. They also developed two univariate models for comparison purposes. In this study, they collected 32 hours of video data from two signalized intersections located in British Columbia, Canada. Then they extracted SSMs, including PET and TTC, using an automated traffic conflict analysis system. Results showed that the developed bivariate models improved crash estimations in terms of precision and accuracy. In 2020, Fu et al. (2020) proposed an extreme value modeling approach with a multivariate Bayesian hierarchical structure in order to estimate rear-end crash frequency at intersections. To achieve this goal, the authors collected 24 hours of video data at four intersections located in British Columbia, Canada. Then they extracted traffic conflicts, including MTTC, PET, and DRAC, using computer vision techniques. Based on the obtained results, it was shown that the trivariate Bayesian hierarchical extreme value model had the best performance compared with other bivariate and univariate models. Recently, Arun et al. (2021) estimated the severe crashes and non-severe crashes frequency by jointly modeling crash frequency's indicators using bivariate extreme value modeling. In this study, TTC, modified TTC (MTTC), and predicted by post-collision change in velocity (Delta-V) were considered as traffic conflict indicators. Data collection was done in Brisbane, Australia, for two days, 12 hours each day. Two bivariate and univariate models were applied. The result denoted that the bivariate approach outperformed the univariate models in terms of crash estimation precision and better fit to the data.

A summary of reviewed studies is provided in Table 1.

Table 1 Summary of the reviewed studies

Ref. (Year)	SSM	Data Collection Method	Data Duration (hours)	# of Locations	Analysis Method	City, Country
Saunier et al. (2010)	rear-end, side, parallel, and head-on interactions, TTC	video-based approach	NA	NA	a refined probabilistic framework for road-user interactions	Kentucky
Alhajyaseen (2015)	PET, angle of collision, and total kinetic energy change	image-processing program "TrafficAnalyzer"	15.5	5	proposed safety measure (ci)	Nagoya, Japan
Zangenehpour et al. (2016)	PET	video-based approach	90	23	ordered logit models	Montreal, Canada
Xie et al. (2016)	TTC	computer vision techniques, video-based approach	70	2	dirichlet process gaussian mixture model (dpgmm)	Brooklyn, NY
30Chen et al. (2017)	RTTC, PET	unmanned aerial vehicle video	1	1	NA	Beijing, China
Wang et al. (2018)	PET	VISSIM by using SSAM	40	10	extreme value theory	Fengxian District, Shanghai
Scholl et al. (2019)	PET	BriskLUMINA	4 months	5	NA	Bolivia
Zheng et al. (2019)	TTC, MTTC, PET, DRAC	computer vision techniques	7	4	bivariate extreme value model	British Columbia, Canada

Zheng and Sayed (2019)	PET, TTC	automated traffic conflict analysis system	32	2	bivariate extreme value models	British Columbia, Canada
Xie et al. (2019)	TTC	automatic vehicle trajectory extraction	70	2	hidden markov models	New York City
Fu et al. (2020)	MTTC, PET, and DRAC	computer vision techniques	24	4	multivariate bayesian hierarchical extreme value model	British Columbia, Canada
Yang et al. (2021)	RS	Connected vehicle data	1 month	14 (corridors)	a structural equation model	Ann Arbor, Michigan
Nadimi et al. (2021)	Several SSMs such as TTC, MTTC, Gap time (GP)	Microscopic traffic data	15 minutes	1 (Interstate)	CP and Pearson correlation coefficient and t-test for comparison	Emeryville, San Francisco
Arun (2021)	TTC, MTTC, Delta-V	deep neural network-based automated conflict extraction method	24	2	bivariate and univariate extreme model	Brisbane, Australia

Findings

According to the comprehensive literature review conducted over the past years, the following findings were obtained:

- Surrogate measures have been extensively used for evaluating the safety of intersections.
- PET and TTC are two of the most commonly used SSMs for safety analysis.
- In recent decades, different research studies have developed and implemented different video-based data collection methods.
- The majority of the available studies have integrated a computer vision-based approach for extracting traffic conflicts from video data.
- In terms of the modeling, different studies used different statistical methods for the purpose of intersection safety analysis.
- Many studies developed safety assessments by estimating the crash frequencies at intersections.
- Recently, researchers suggested extreme value analysis for integrating traffic conflicts in frameworks to estimate crash frequencies at intersections.

CHAPTER 3. METHODOLOGY

3.1 Data Collection

For evaluating the performance of the developed safety analytics tool, nine hours of continuous video data were collected from six different signalized intersections on Delsea Dr., Glassboro, New Jersey. Delsea Dr. is one of the segments of a state highway, Route 47, located in the southern part of New Jersey. Along the segment, several signalized and unsignalized intersections are built to improve the safety and mobility of the road users in Gloucester County, New Jersey. Table 2 provides brief information about the selected study locations and the video data collection schedules. Figure 1 shows the intersection locations on the map. The nine hours of video data were recorded with a 2704 X 1520 resolution using a Go Pro Hero 9 at 30 Frames Per Second (FPS).

Table 2 Description of study locations and data collection schedules

#	Location	Intersection Type	Date	Timing
1	Delsea Dr. N and Greentree Rd.	3-Leg Intersection	09/10/2021	9:00 AM to 6:00 PM
2	Delsea Dr. N and Fishpond Rd.	3-Leg Intersection	09/10/2021	9:00 AM to 6:00 PM
3	Delsea Dr. N and West St.	3-Leg Intersection	09/10/2021	9:00 AM to 6:00 PM
4	Delsea Dr. N and High St.	4-Leg Intersection	09/14/2021	9:00 AM to 6:00 PM
5	Delsea Dr. N and Donald Barger Blvd.	4-Leg Intersection	12/14/2021	9:00 AM to 6:00 PM
6	Delsea Dr. N and New St.	4-Leg Intersection	09/7/2021	9:00 AM to 6:00 PM

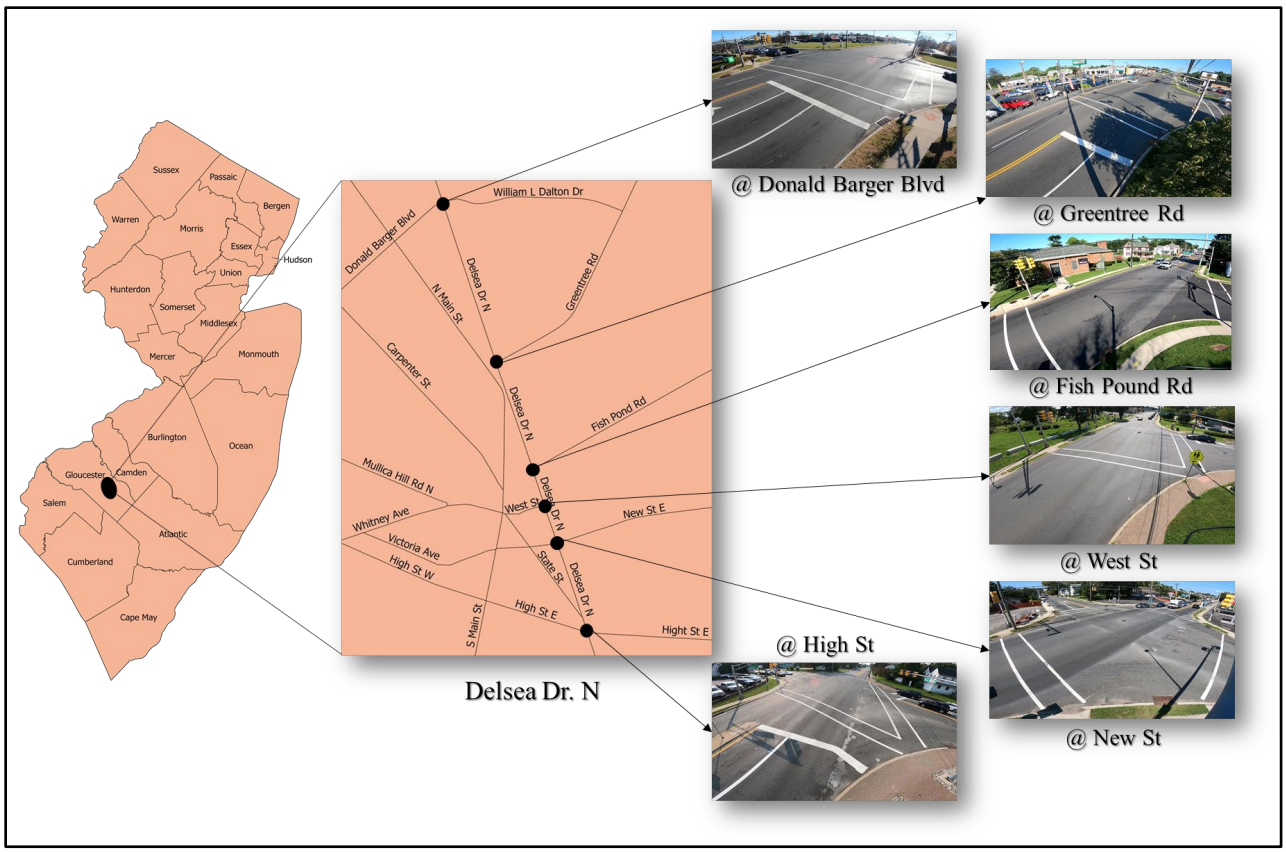

Figure 1 Study Intersections

3.2 Detection & Tracking

Real-time object detection and tracking algorithms have been widely used to achieve traffic management objectives and evaluate traffic safety. This main goal of this algorithm is to locate the positions (i.e., X, Y coordinates) and the moving objects' size in a video or an image. Detecting an object is an initial step in all detection and tracking methodology. In this project, the Yolo-V5 (You Only Look Once) Algorithm and a COCO dataset were integrated to detect cars, trucks, buses, bicyclists, and pedestrians from the video (Jocher et al., 2021; Lin et al., 2014).

YOLO algorithm is a deep learning network for real-time detection that performs its main two tasks in a series pattern. The algorithm first identifies the location of the object pixels, and then based on the pre-trained weights, it classifies the object. YOLO considers the image pixel values as the inputs and predicts the object's bounding boxes and class probability as an output result. The algorithm uses only a single neural network to perform the tasks at a high processing speed. YOLO-V5 is built on a PyTorch framework instead of the original Darknet framework used in the previous version (Redmon et al., 2016; Redmon et al., 2018; Jocher et al., 2021).

Figure 2 shows the process principle of the YOLO algorithm. First, the algorithm takes a frame/image as an input and divides it into NxN grids. Then, each cell in the grid is processed to predict the bounding box for all the objects in a frame. Simultaneously, it looks for the class

probabilities for the identified bounding boxes. Lastly, each bounding box provides X & Y coordinates, height & width, confidence score, and the class value. As a part of this study, we have considered the detection confidence score threshold to be 80 percent.

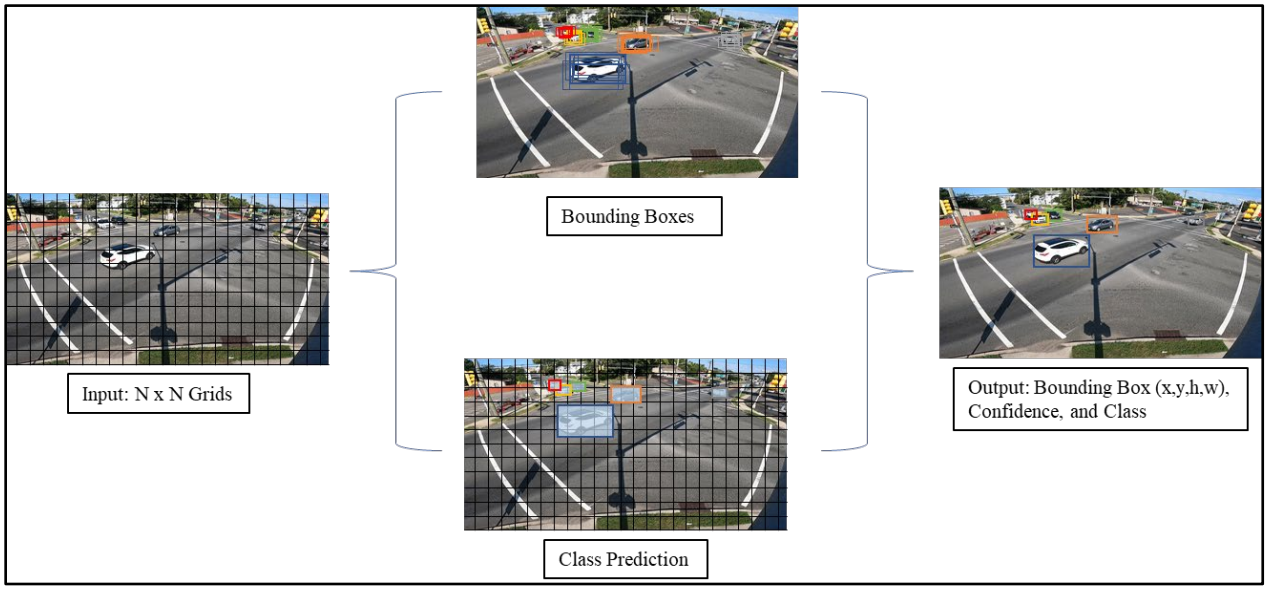

Figure 2 YOLO Algorithm process flow chart

Regarding processing speed, YOLO-V5 archives the inference time as fast as 0.007 seconds per image for 140 FPS video while upholding detection accuracy like previous versions. YOLO-V5 has a weight file of 27 MB, which is 90 percent smaller than previous versions. Optimized YOLO-V5 is based on PyTorch and can be easily compiled to ONNX and CoreML to make mobile deployment easy. Overall, using YOLO-V5, detection can be carried out in a wider area with fewer space constraints (Wang et al., 2020).

The second step of detection and tracking methodology is object tracking. Object tracking has been recognized as the most critical task in all computer vision projects. Extensive research has been conducted for visual object tracking; however, there have been many difficulties in handling changes in tracking the detected object. For instance, occlusion, changes in bounding box dimension, variation in illuminations, camera motion, etc., cause many errors in tracking. As part of this study, DeepSORT, a Simple Online and Real-Time Tracking (SORT) algorithm, is used for tracking multiple objects frame by frame. DeepSORT uses the Hungarian and Kalman filter algorithm to track a detected object (Bewley et al., 2016). The baseline process flow of the DeepSORT algorithm can be described as follows (Hou et al., 2019):

- **Track Estimation:** A DeepSORT algorithm uses the Kalman Filter method to predict the position of the object bounding box in the current frame. DeepSORT uses a standard version of the Kalman Filter that considers the constant velocity and linear regression. Spatial information is only used by the track estimation, i.e., the X and Y coordinates of the bounding box.

- **Appearance Descriptor:** An appearance descriptor is used to attain the detection and tracks appearance details. It is a pre-trained Convolutional Neural Network (CNN) of a massive scale of re-identification dataset. Wherein the network can identify the features that are similar to previously detected objects and/or far away from each other.
- **Data Association:** Further, based on the track estimation and appearance descriptors results, it is possible to see the correlation between the old and newly detected objects' current frames. Remarkably, the DeepSORT algorithm uses a detection confidence threshold to filter out all detection. The algorithm also uses the cost matrix to represent spatial and appearance similarities between existing and new detection tracks. As a focus of this study, IOU_machting, NN_matching, class, and average detection confidence threshold functions were used to improve the accuracy of the tracking algorithm.
- **Track Handling:** The objects tracked from the data association are taken care of during the track handling. For instance, if the newly tracked object is not associated with the old tracks, then the track will be tentatively held until it does not satisfy all the conditions for getting a new track ID. Once it satisfies all the requirements, then a new track ID is updated. Otherwise, the tentative track will be removed

3.3 Conversion of Pixel Coordinates and Speed Estimation

Estimating the position and speed of road users is a challenging problem in video analytics. The study applies the scale factor conversion to address this problem by calculating the pixel per meter according to the camera perspective. The first frame is extracted from a given video data and is divided into eight equal sections to identify the distribution of road features and markings. Second, using the road features and markings on the frame, several horizontal lines are drawn on the frames, and the pixel distance between the start and endpoint of the line is calculated using the python OpenCV library. Third, the same lines are drawn on google map with reference to road features and markings, and meter distance is evaluated. Lastly, the pixel per meter value is calculated for each horizontal line by using Equation 1 as follows:

$$Pixel\ Per\ Meter\ = \frac{Pd_{(x_1,y_1):(x_n,y_n)}}{Md\ (m)} \quad (1)$$

where:

$Pd_{(x_1,y_1):(x_n,y_n)}$: is the distance between the start and endpoint of the horizontal line drawn on the frame in coordinates

$Md\ (m)$: is the distance between the start and endpoint of the line drawn on the google map in meters

It should be noted that an average pixel per meter value is considered for each section to convert the pixel coordinates.

Figure 3 demonstrates eight sections on the frame and matching horizontal lines with the google map for one of the study locations.

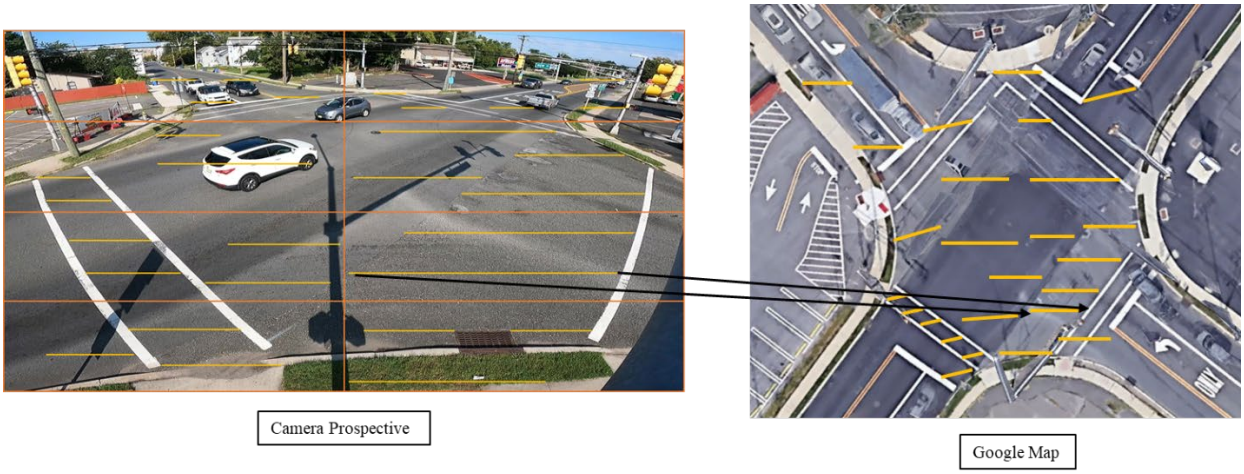

Figure 3 Pixel Coordinate matching with Google map

3.4 Traffic Counts

As the scope of this study, a system to identify the traffic flow that counts and classifies the vehicle base on the direction flow was developed. As discussed previously, detection and tracking of the vehicle were extracted using YOLO-V5 and DeepSORT algorithm. Furthermore, to obtain the flow direction of the vehicles, predefined zones were created for each location. Wherein each unique pixel value from the zone was extracted and matched with the complete trajectories extracted from the model. Figure 4 represents the zones that are created using the OpenCV library and polygon plotting method. The flow direction of the completely tracked objects was determined based on the start and endpoints of each track ID.

(Location: Delsea Dr. N and Donald Barger Blvd)

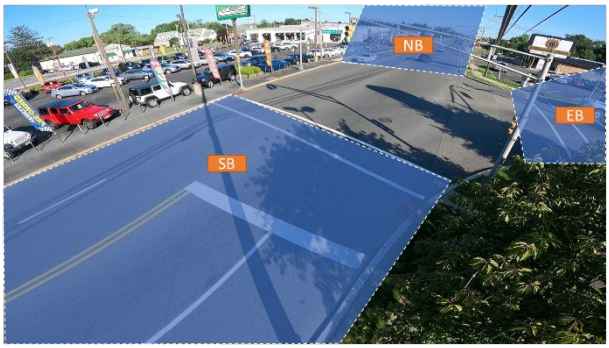

(Location: Delsea Dr. N and Greentree Rd.)

(Location: Delsea Dr. N and Fishpond Rd.)

(Location: Delsea Dr. N and West St.)

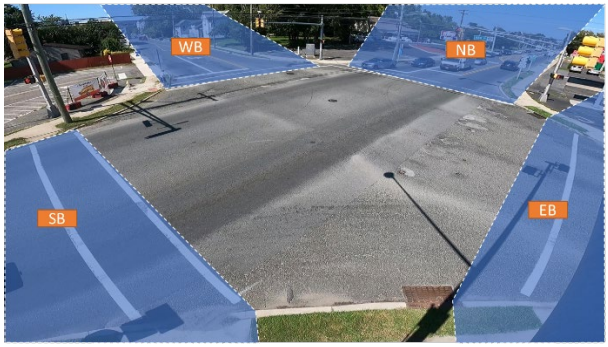

(Location: Delsea Dr. N and New St.)

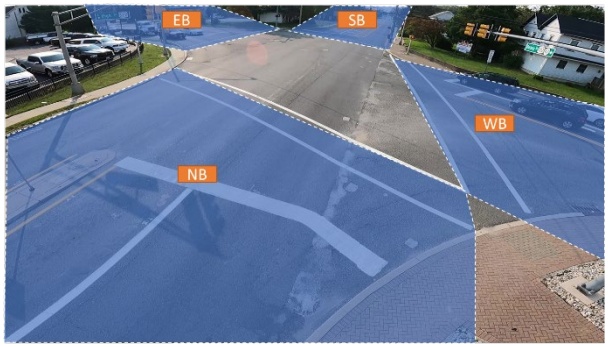

(Location: Delsea Dr. N and High St.)

Figure 4 Predefined zones at the study intersection

3.5 Traffic Non-Compliance Counts

Traffic non-compliance counts such as vehicles running red lights and pedestrian jaywalking events are crucial concerns at a signalized intersection. One element of the safety analytics tool was developed to identify vehicles that were running red lights. A predetermined traffic light region must be chosen, and a correnspondingand adjacent violation bars must be drawn on the frame. During the signal's red phase, vehicles passing the correnspondingviolation bar are considered as vehicles running red light events. While during the signal's green phase, vehicles passing the adjacent violation bar are considered as vehicles running red light events. Additionally, if the intersection has a sign mentioning “NO TURN ON RED,” then configurations can be made by integrating the directional traffic data and deciding on the redlight running light. Figure 5 shows the position of the violation bars and traffic lights for the study locations.

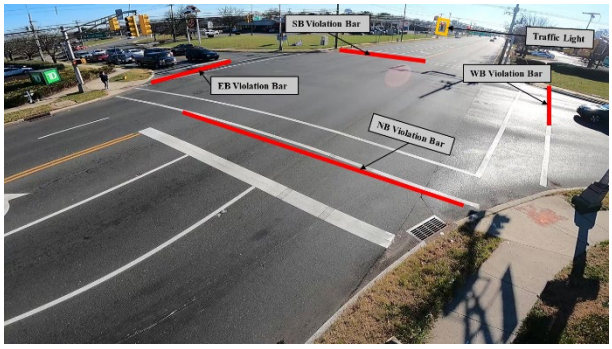

(Location: Delsea Dr. N and Donald Barger Blvd.)

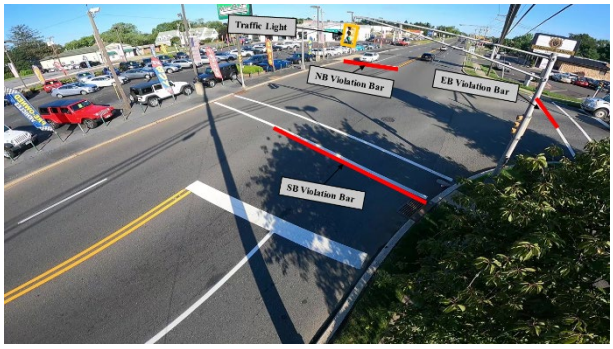

(Location: Delsea Dr. N and Greentree Rd.)

(Location: Delsea Dr. N and Fishpond Rd.)

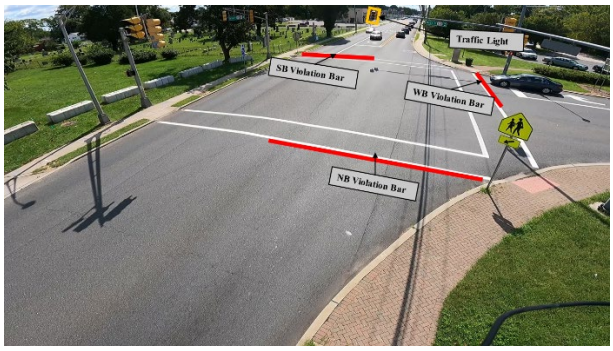

(Location: Delsea Dr. N and West St.)

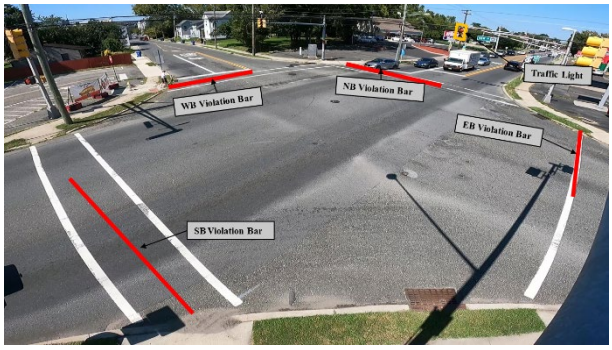

(Location: Delsea Dr. N and New St.)

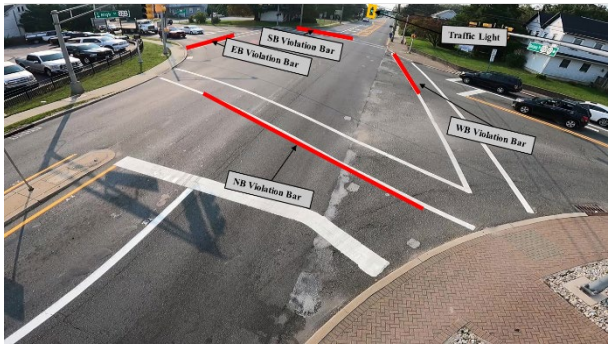

(Location: Delsea Dr. N and High St.)

Figure 5 Positions of the violation bars and traffic lights

In terms of pedestrian jaywalking events, another module of the analytics tool that functions using the python OpenCV library and polygon plotting function was developed. A predefined region is created on the frame covering all of the crosswalks and the sidewalk areas. Then, a condition algorithm is deployed that continuously verifies the extracted trajectory data of the pedestrians. For instance, if any coordinate values were observed outside the region, it was considered a jaywalking event. Figure 6 indicates the predefined polygon region created on the frame for the two intersections.

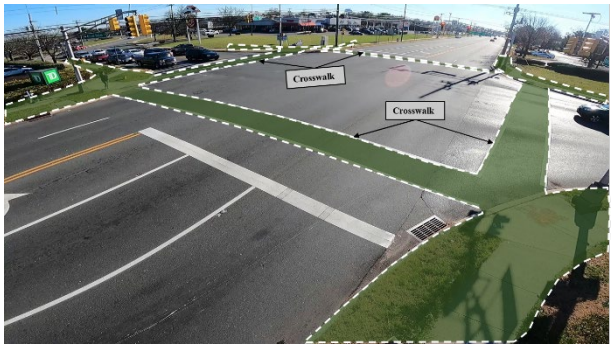

(Location: Delsea Dr. N and Donald Barger Blvd.)

(Location: Delsea Dr. N and Greentree Rd.)

(Location: Delsea Dr. N and Fishpond Rd.)

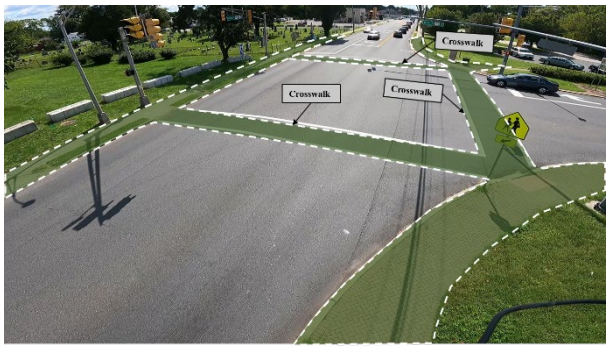

(Location: Delsea Dr. N and West St.)

(Location: Delsea Dr. N and New St.)

(Location: Delsea Dr. N and High St.)

Figure 6 Polygon region for identifying the Jaywalking event

3.6 Surrogate Safety Measures

SSM is one of the widely used approaches for identifying future threats and evaluating safety. Each SSM is calculated based on the occurrence of conflict events between two road users. Conflict is defined as an observable point, line, or an area where two or more road users intersect in time and space with a possibility of colliding with each other if the speed and direction of both road users remain unchanged (Amundsen and Hyden, 1977). SSMs are considered as the best safety evaluation method that help identify the near-miss conflict events at the study location and compare the results with the historical crash data to recommend countermeasures. There are

several SSMs that are used for evaluation, including TTC, PET, Maximum Speed, Speed difference, and deceleration rate. As a part of this study, PET and TTC were considered as the SSMs for evaluating the traffic conflicts for the turning vehicles at the intersections for analysis.

PET

PET can be defined as "the time difference between the moment an "offending" vehicle passes out of the area of a potential collision and the moment of arrival at the potential collision point by the "conflicted" vehicle possessing the right-of-way" (Cooper and Ferguson, 1976). PET's calculation does not need extrapolation of future positions or parameters related to speed. In terms of processing the trajectory data, PET is calculated as a function of the paired vehicles. A time-space diagram to calculate the PET for vehicle-to-vehicle conflict is represented in Figure 7.

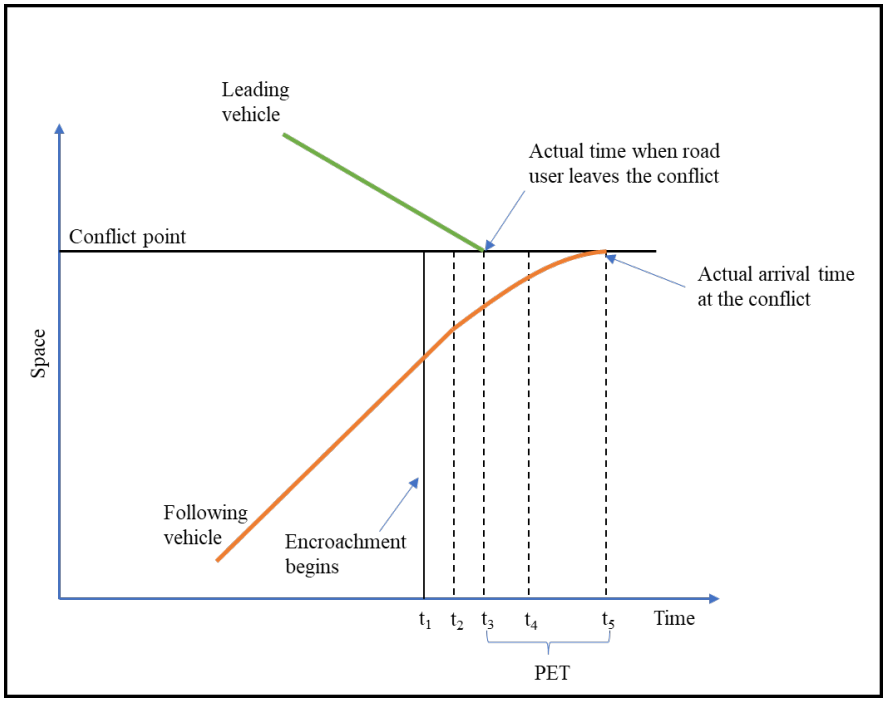

Figure 7 Time-space diagram to identify the PET

PET for paired vehicles at a conflict point is obtained as:

$$PET_t = t_{F,t} - \ t_{L,t} \quad (2)$$

Where
$t_{F,t}$: the time when the following vehicle arrives at a conflict point
$t_{L,t}$: the times the leading vehicle leaves at a conflict point

As a part of this study, the extracted trajectory, bounding box centroid, bottom-front, and the bottom-back (i.e., the front and the rear of the vehicle) points were calculated and considered for the conflicting vehicle. Similar to the previous studies, PETs with less than 5 seconds and less than

1.5 seconds were considered potential conflict and dangerous conflict, respectively. (Zangenehpour et al., 2015; Fu. et al., 2016). Additionally, the study also considered the 20 seconds as the arbitrary threshold for identifying all potential risks for vehicle-to-vehicle collisions at the intersections.

TTC

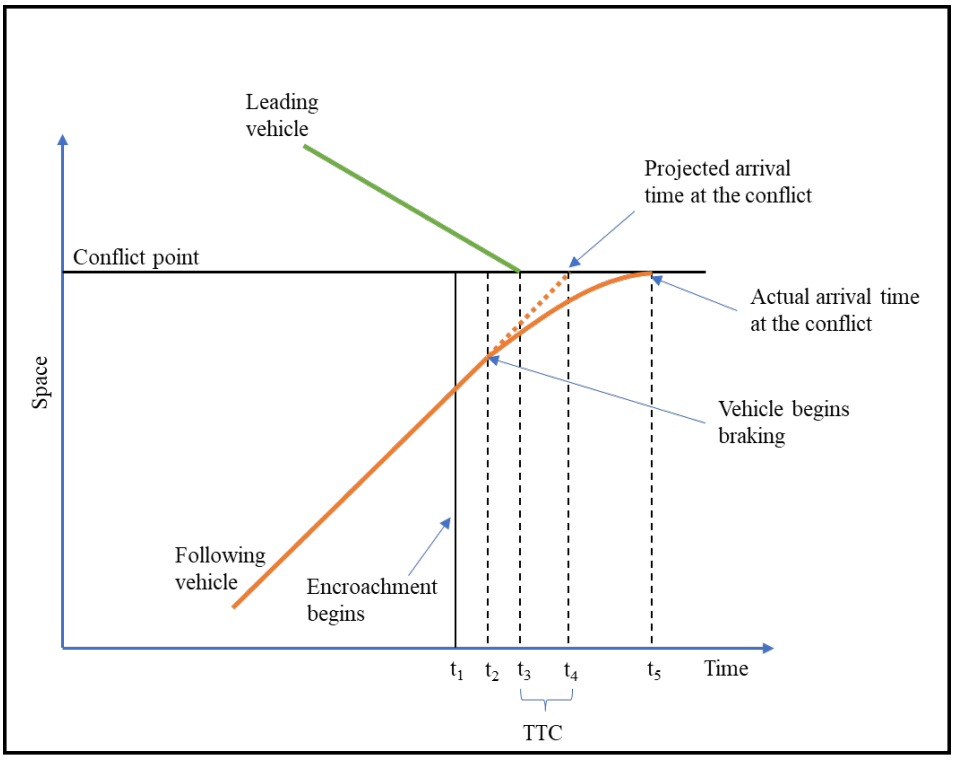

Figure 8 Time-space diagram to identify the TTC

The collision time required for two vehicles if they keep driving at the same speed and the same path is defined as TTC (Hayward, 1972). As discussed previously, the extracted trajectory, bounding box centroid, bottom-front, and the bottom-back (i.e., the front and the rear of the vehicle) points were calculated and considered for the conflicting vehicles. First, the intersecting point between the two trajectories was identified, i.e., the conflict point. Then based on the conflicting point, the vehicle that arrived first at the conflict point is assigned as the leading vehicle, and the vehicle that arrived second is considered as the following vehicle. After identifying the leading and the following vehicles, the trajectory data for the following vehicle is reconstructed to reach the same conflict point following a similar path but at a different speed, which was observed before the deceleration occurred. With this process, the reconstructed trajectory will provide a projected arrival time for the following vehicle, and then TTC can be determined using the equation 3. A time-space diagram to calculate the TTC for vehicle-to-vehicle conflict is represented in Figure 8

$$TTC_t = t_{F,t"} - \ t_{L,t} \quad (3)$$

where:
$t_{F,t"}$: the projected arrival time of the following vehicle at a conflict point after reconstructing the trajectory.
$t_{L,t}$: the times the leading vehicle leaves at a conflict point

For this study, TTC values that provided a negative time difference were not considered for identifying the severity.

3.7 Intersection Safety Analysis

As mentioned earlier, in recent years, the EVT has been extensively implemented as a powerful tool in many areas of research to investigate the distributions of extreme events. The extreme value distribution is generally comprised of two families to analyze extreme events. The first family, known as Generalized Extreme Value (GEV), aggregates the observations into fixed time or space intervals and takes the maxima of each single block. This approach is called block maxima (BM). The second family, also known as Generalized Pareto Distribution (GPD), takes the observations over a predefined threshold as the extremes. This approach is called as peak over threshold (POT). In this study, the main focus will be on the application of GEV using BM approach for intersection safety evaluations.
Assume that $X_1, X_2, X_3, \ldots, X_n$ represent a set of independent random variables following an unknown distribution function as $F(x) = \Pr(X_i \leq x)$, and M_n represents block maxima indicating the maximum of the independent random variables in each block. When n approaches infinity ($n \to \infty$), M_n converges to a GEV distribution formulated as follows (Zheng and Sayed, 2019a):

$$F(x) = \exp\{-\left[1 + \xi\left(\frac{x-\mu}{\sigma}\right)\right]^{-\frac{1}{\xi}}\} \quad (4)$$

where:
$-\infty < \xi < +\infty$: Shape parameter
$\sigma > 0$: Scale parameter
$-\infty < \mu < +\infty$: Location parameter

In the present study, GEV distribution with BM approach is implemented to predict the crash risk at intersections. The risk of the crash is defined as observing a negated value of an event (e.g., PET or TTC) that is equal to or more than zero. It should be mentioned that the negated PET or TTC is considered for determining BM. Given the above information, one can calculate the risk of the crash using the following equation (Zheng and Sayed, 2019a):

$$CR = \Pr(D \geq 0) = 1 - F(0) = 1 - \exp\{-\left[1 + \xi\left(\frac{x-\mu}{\sigma}\right)\right]^{-\frac{1}{\xi}}\} \quad (5)$$

where:

CR: Crash risk
D: the negated PET or negated TTC

The calculated *CR* from equation (5) is a non-negative value. CR can be considered as the crash frequency corresponding to the time period (*t*) from which the traffic conflicts are collected. By supposing that the *t* is a representative of a period of interest denoting with *T*, the crash frequency that occurred during the *T* period can be computed as:

$$N = \frac{T}{t} CR \tag{6}$$

where:
N: number of crashes during the time period *T*

In Equation 6, *T* period is longer than the *t* period. It should be mentioned that the number of extracted PET and TTC data for 3-leg intersections was low. Hence, only 4-leg intersections were used to develop the GEV models for yearly crash estimations. Once the number of crashes is estimated for each location, the next step would be ranking the intersections. EPDO is a commonly used crash ranking method that is based on weighting by crash severities (Lim and Kweon, 2013). In this method, different weights are assigned to crashes with different severity levels in order to convert them equivalent to property damage only crash, known as EPDO score. The EPDO score for each location can be calculated using the following equation:

$$EPDO_n = \sum_s W_s \times C_{s,n} \tag{7}$$

where:
n: location number
$EPDO_n$: EPDO score for location n
s: Severity level
W_s: Weight assigned to crashes with the severity level *s*
$C_{s,n}$: Number of crashes with the severity level *s* occurred at location *n*

In this project, as the final step, the considered locations were ranked based on the calculated EPDO score. The lower the EPDO score, the safer the locations are. It should be mentioned that the severity distribution of the left-turn crashes for the entire New Jersey was used to calculate the ratios for each severity level. To this end, five years of left-turn crashes (2015 to 2019) occurred in New Jersey as well as their severity were obtained. Thereafter, the ratio of each severity level over total crashes was determined for each year. Finally, the ratios were averaged for the total study period of crashes considered in this study.

CHAPTER 4. RESULTS

As a part of this study, 54 hours of high-resolution (2704 X 1520) video data consisting of more than 5.8 million frames were processed using the AI and a web-based Safety Analytics application. Nearly 112,000 road users were detected, and trajectory data was extracted to assess the intersection safety. To assess the overall safety of intersections, the directional volume of vehicles, red light running of vehicles, jaywalking for pedestrians, TTC, and PET events for turning vehicles were identified. Additionally, by using the PET and TTC, EVT models were developed to predict crash frequencies at the 4-leg intersections. Eventually, EPDO score was calculated, and the 4-leg intersections were ranked according to their EPDO value.

4.1 Detection and Tracking Accuracy

First, detected and tracked data was validated by comparing the result of 60 minutes of video with manually counted data for all the intersections. Table 3 shows the relative accuracy and the error by comparing the values of detected and manual counts for each location with respect to the starting direction. Based on the results, it can be seen that the accuracy values above one represent more vehicle counts predicted by the algorithm than the actual vehicle. In contrast, the values below one represent that the algorithm predicted a lower vehicle count than the actual counts. Error is the absolute value calculated by subtracting the accuracy from one, depicting a detailed validation result for each intersection leg.

Overall, it was observed that the detection and tracking algorithm implemented in the developed application showed an error between 0.01 to 0.08, representing an accuracy between 92 and 99 percent. The intersections at Donald Barger Blvd., Greentree Rd., Fishpond Rd., West St., and New St. showed an accuracy close to one with an error value of 0.04, 0.02, 0.02, 0.01, and 0.04, respectively. These results show that the detection and tracking algorithm performed well for most of the intersections, with an accuracy above 95 percent. However, the results for High St. intersection represented a 0.08 error which was slightly higher than other locations. For the High St. intersection, it was observed that the major detection and tracking loss was observed at the south leg of the intersection, which was far from the camera mounting pole.

Table 3 Detection and tracking accuracy results for all locations

Delsea Dr. N and Donald Barger Blvd.				
Start Direction	**Detection Counts**	**Manual Count**	**Accuracy**	**Error**
North	767	786	0.98	0.02
South	863	782	1.10	0.10
East	436	417	1.05	0.05
West	186	186	1.00	0.00
Total	2252	2171	1.04	0.04
Delsea Dr. N and Greentree Rd.				
Start Direction	**Detection Counts**	**Manual Count**	**Accuracy**	**Error**

North	678	738	0.92	0.08
South	1120	1026	1.09	0.09
East	309	309	1.00	0.00
West	0	0	-	-
Total	2107	2073	1.02	0.02
Delsea Dr. N and Fishpond Rd.				
Start Direction	**Detection Counts**	**Manual Count**	**Accuracy**	**Error**
North	773	788	0.98	0.02
South	1088	1031	1.06	0.06
East	297	291	1.02	0.02
West	0	0	-	-
Total	2159	2110	1.02	0.02
Delsea Dr. N and West St.				
Start Direction	**Detection Counts**	**Manual Count**	**Accuracy**	**Error**
North	904	850	1.06	0.06
South	887	984	0.90	0.10
East	0	0	-	-
West	569	552	1.03	0.03
Total	2360	2386	0.99	0.01
Delsea Dr. N and New St.				
Start Direction	**Detection Counts**	**Manual Count**	**Accuracy**	**Error**
North	848	921	0.92	0.08
South	880	759	1.16	0.16
East	488	461	1.06	0.06
West	290	278	1.04	0.04
Total	2505	2419	1.04	0.04
Delsea Dr. N and High St.				
Start Direction	**Detection Counts**	**Manual Count**	**Accuracy**	**Error**
North	898	846	1.06	0.06
South	458	644	0.71	0.29
East	372	404	0.92	0.08
West	347	371	0.93	0.07
Total	2075	2265	0.92	0.08

4.2 Direction-based Traffic Count

Besides total detected and tracked vehicles, a directional-based traffic count was extracted by defining the zone parameters during the analysis. Table 4 demonstrates the directional traffic count by identifying the starting and ending points of the detected trajectories for the six locations. Start and endpoints for each completely tracked vehicle are extracted and matched with the zone parameter to determine the flow direction. Overall the result showed that most of the vehicles entered the intersections from North or South leg for all the intersections, which represents the traffic flow on the Delsea Dr. N route. Note that intersections at Greentree Rd., Fishpond Rd., and

West St. are the 3-leg intersections, which shows zero value for the direction where the zone was not created. For instance, to interpret the result for the intersection at Donald Barger Blvd, the value 2043 in Table 4 demonstrates that 2043 vehicles entered the intersection from South and exited the intersection from North.

Table 4 Direction-based traffic count for all locations

Delsea Dr. N and Donald Barger Blvd.					
Direction	**North**	**South**	**East**	**West**	**Total**
North	0	5188	2471	1670	9329
South	2043	0	546	2108	4697
East	877	1432	0	3043	5352
West	1653	815	2058	0	4526
Total	4572	7435	5075	6821	23904
Delsea Dr. N and Greentree Rd.					
Direction	**North**	**South**	**East**	**West**	**Total**
North	0	5032	419	0	5452
South	7013	0	1455	0	8467
East	604	1690	0	0	2294
West	0	0	0	0	0
Total	7616	6723	1874	0	16213
Delsea Dr. N and Fishpond Rd.					
Direction	**North**	**South**	**East**	**West**	**Total**
North	0	5826	342	0	6168
South	7397	0	853	0	8250
East	748	1118	0	0	1866
West	0	0	0	0	0
Total	8144	6944	1196	0	16284
Delsea Dr. N and West St.					
Direction	**North**	**South**	**East**	**West**	**Total**
North	0	5559	0	1776	7334
South	5288	0	0	1926	7215
East	0	0	0	0	0
West	2419	1930	0	0	4349
Total	7708	7489	0	3702	18898
Delsea Dr. N and New St.					
Direction	**North**	**South**	**East**	**West**	**Total**
North	0	4426	1381	452	6259
South	6643	0	588	207	7439
East	1787	654	0	1037	3479
West	472	186	1455	0	2113
Total	8903	5267	3423	1697	19290
Delsea Dr. N and High St.					
Direction	**North**	**South**	**East**	**West**	**Total**
North	0	4435	2132	1619	8186
South	2181	0	138	453	2772
East	1691	349	0	1513	3553
West	798	528	1364	0	2690

Total	4670	5312	3634	3585	17201

4.3 Traffic Non-Compliance Counts

When understanding the safety of an intersection, non-compliance behaviors of the road users are imperative evaluation paraments. As part of this study, the rate of non-compliance for the vehicles examined by extracting the redlight running events, while the rate of noncompliance for pedestrians was analyzed by extracting jaywalking events for all junctions.

Vehicles - Redlight Running Events

The non-compliance events for the vehicle have been calculated. To calculate the vehicle-based non-compliance events, running red light vehicles were identified by detecting one of the traffic lights at the intersection and creating a virtual violation bar that corresponds with the signal phase for the same direction flow. While for the other directions, a negation logic was implemented for the detected traffic signals phase to extract red light running events. Table 5 demonstrates the results of the detected redlight running events for nine hours at each study location. As can be seen in this able, the intersections at New St. and High St. represented the highest rate of non-compliance, i.e., 0.008 and 0.007 percent, respectively. It is worth noting that both locations had no right turn on red signs installed, not permitting drivers to make a right turn during red, which may have been ignored the majority of the times. Figure 9 illustrates the detected vehicle non-compliance event at the Donald Barger Blvd. intersection.

Table 5 Detection results: Vehicle non-compliance counts (Redlight Running Events)

Location	Total Vehicle Counts	Vehicle Non-compliance Counts	Rate of Non-Compliance
Delsea Dr. N and Donald Barger Blvd.	23904	21	0.0009
Delsea Dr. N and Greentree Rd.	16213	24	0.0015
Delsea Dr. N and Fishpond Rd.	16284	28	0.0017
Delsea Dr. N and West St.	18898	30	0.0016
Delsea Dr. N and New St.	19290	157	0.0081
Delsea Dr. N and High St.	17201	132	0.0077
Total	111790	392	0.0035

Figure 9 An illustration of a detected vehicle redlight running event

Pedestrians – Jaywalking

For extracting pedestrian non-compliance events, pedestrians not using the crosswalk for crossing the street or jaywalking are considered as non-compliance events. Based on aggregated results for all the locations, it can be observed that 1 in 4 pedestrians that crosses the street is not entirely using a crosswalk to cross the street or is jaywalking. To be specific, the intersections at High St. and Greentree Rd. had the highest rate of non-compliance events detected, i.e., 0.43 and 0.35 percent, respectively. Table 6 demonstrates the results of the non-compliance rate of detected pedestrians for nine hours at each study location. Figure 10 illustrates a detected pedestrian non-compliance event at the High St intersection.

Table 6 Detection results: Pedestrian non-compliance counts (Jaywalking)

Location	Total Pedestrian Counts	Pedestrian Non-compliance Counts	Rate of Non-Compliance
Delsea Dr. N and Donald Barger Blvd.	91	20	0.22
Delsea Dr. N and Greentree Rd.	101	35	0.35
Delsea Dr. N and Fishpond Rd.	113	30	0.27
Delsea Dr. N and West St.	102	17	0.17
Delsea Dr. N and New St.	194	46	0.24
Delsea Dr. N and High St.	94	40	0.43
Total	695	188	0.27

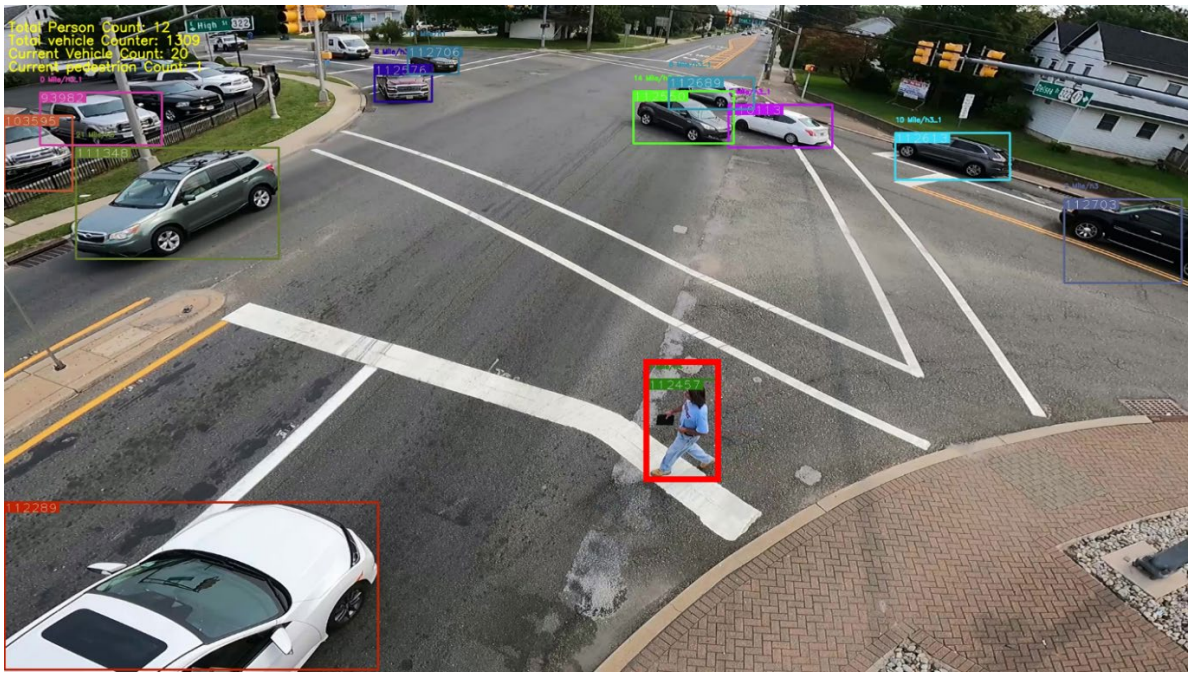

Figure 10 An illustration of a detected pedestrian jaywalking event

4.4 Surrogate Safety Measures

PET and TTC are SSMs used in this study to identify the conflicts for the left-turning vehicles and evaluate the severity of each interaction. For accessing the PET and TTC, nearly 120000 complete trajectory data for all the locations were extracted. The trajectories with conflicts of less than 20 seconds were considered to ease the further calculations in this study.

PET

The trajectories with conflicts of less than 20 seconds were considered to identify possible and dangerous conflicts using Equation 2. PET less than 1.5 seconds demonstrates a higher probability of a crash occurrence and a dangerous conflict. At the same time, a PET event between 1.5 and 5 seconds is a possible conflict (Zangenehpour et al., 2015; Fu. et al., 2016. Table 7 depicts the analyzed PET results for nine hours of video data for each study location. Among all the 3-leg intersections, the intersection at Fishpond Rd. showed a higher percentage of the dangerous conflicts compared to other locations, i.e., 24.1 percent of the possible conflicts were less than 1.5 seconds. On the other hand, for the 4-leg intersections, the intersection at New St showed a higher percentage of the dangerous conflicts compared to other locations, i.e., 12.1 percent of the possible conflicts were less than 1.5 seconds. Note that the frequency of conflicting events is heavily dependent on the left-turning volume.

Table 7 Analysis result for PET

PET Threshold (Seconds)	PET Event Count						Description
	Delsea Dr. N and Donald Barger Blvd.	***Delsea Dr. N and Greentree Rd.***	***Delsea Dr. N and Fishpond Rd.***	***Delsea Dr. N and West St.***	***Delsea Dr. N and New St.***	***Delsea Dr. N and High St.***	
PET Events < 20	10991	615	929	1649	4291	2764	Arbitrary Count
PET Events < 5	958	134	191	196	754	438	Possible Conflict
PET Events < 1.5	75	15	46	28	91	36	Dangerous Conflict

TTC

As part of computing TTC values, the reconstructed trajectories after the deceleration was discovered and the events that had conflict less than 20 seconds were analyzed to extract to extract possible and dangerous conflicts using equation 3. Similar to PET, TTC less than 1.5 seconds demonstrates a higher probability of a crash occurrence and a dangerous conflict. While a TTC event between 1.5 and 5 is a possible conflict. Table 8 shows the calculated TTC results for nine hours of video data for each study location. Similar to PET results, TTC data for the 3-leg intersection, Fishpond Rd., and the 4-leg intersection, New St., indicated a larger rate of risky conflicts than other sites, with 27.0 and 14.6 percent possible conflicts were less than 1.5 seconds, respectively.

Table 8 Analysis result for TTC

TTC Threshold (Seconds)	TTC Event Count						Description
	Delsea Dr. N and Donald Barger Blvd.	***Delsea Dr. N and Greentree Rd.***	***Delsea Dr. N and Fishpond Rd.***	***Delsea Dr. N and West St.***	***Delsea Dr. N and New St.***	***Delsea Dr. N and High St.***	
TTC Events < 5	989	136	181	205	794	445	Possible Conflict

TTC Events < 1.5	102	20	49	43	116	42	Dangerous Conflict	

4.5 Intersection Safety Modeling

As mentioned earlier, in order to model the crash risk, a BM approach was implemented in which the traffic conflict indicator (e.g., PET or TTC) is divided into fixed time intervals. The low number of block maxima (large time intervals) would lead to less accurate estimations with large variance. On the other hand, having too many block maxima (small time intervals) may take ordinary traffic conflict observations as extreme events. Hence, choosing an appropriate time interval is a necessity in order to have good model estimations. According to the previous studies, generally, more than 30 time intervals for taking the block maxima are required in order to fit a model (Zheng and Sayed, 2019a; Zheng et al., 2014a). In this study, GEV models with four different block intervals were developed for the three locations (4-leg intersections). Table 9 tabulates the selected number of blocks and the model estimation results for each location. By substituting the estimated parameters from the developed models in Equation 5, the number of yearly crashes for the three locations (4-leg intersections) was estimated. Moreover, a 95% confidence interval (CI) of the estimated crashes was calculated. Table 9 also lists the estimated crashes and their 95% C.I.

Table 9 Estimation results of GEV model

Model	Location	# of Blocks	Estimate			Standard Error			Deviance	Estimated Crashes (95% C.I.)
			μ	σ	ξ	μ	σ	ξ		
GEV_PET	Delsea Dr. N and High St.	32	-1.245	0.976	-0.782	0.192	0.194	0.200	71.326	0.157 (0, 111.2)
	Delsea Dr. N and New St.	56	-1.419	0.927	-0.727	0.134	0.121	0.110	122.302	0 (0, 64.7)
	Delsea Dr. N and Donald Barger Blvd.	37	-1.273	0.727	-0.552	0.136	0.117	0.166	70.839	0.584 (0, 75.7)
GEV_TTC	Delsea Dr. N and High St.	32	-1.315	0.779	-0.563	0.170	0.157	0.259	65.539	1.429 (0, 95.4)
	Delsea Dr. N and New St.	56	-1.020	0.619	-0.658	0.115	0.099	0.144	50.963	0 (0, 74.8)
	Delsea Dr. N and Donald Barger Blvd.	55	-1.409	0.634	-0.404	0.096	0.074	0.114	99.038	1.014 (0, 42.8)

Figures 11 and 12 illustrate the goodness of fit plots for the developed models using PET and TTC. According to the QQ plots, the difference between empirical and model values is very small for

both PET and TTC results. The Density plots also indicate that the models developed using PET and TTC were fitted well.

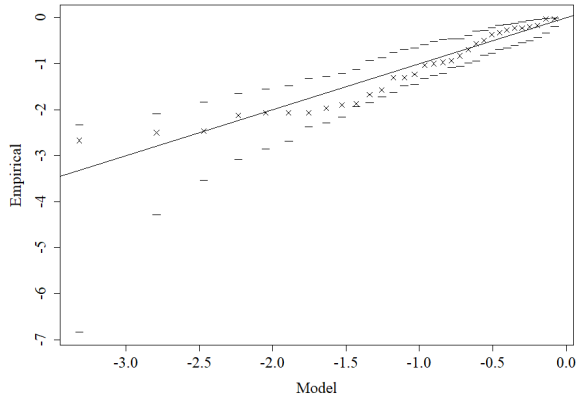

a) QQ plot for Delsea Dr. N and High St.

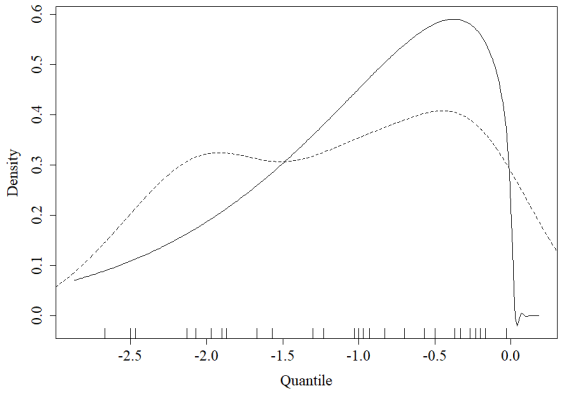

b) Density plot for Delsea Dr. N and High St.

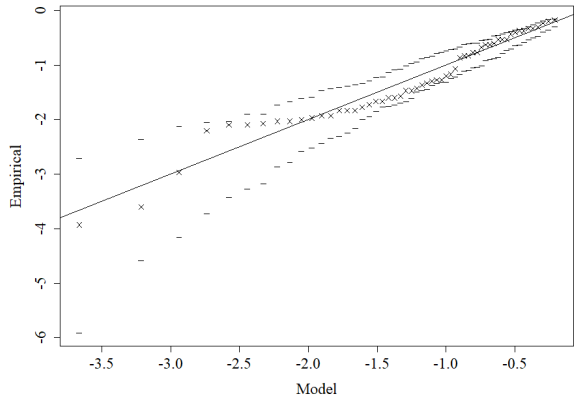

c) QQ plot for Delsea Dr. N and New St.

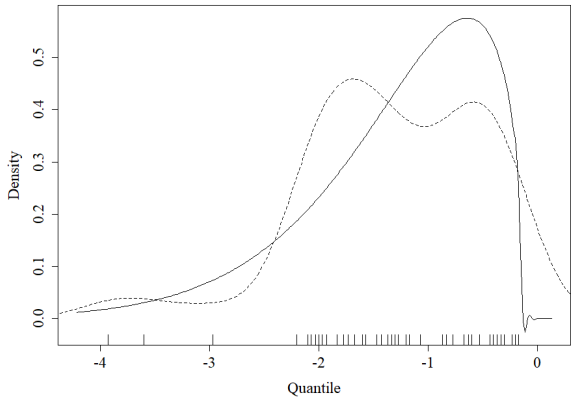

d) Density plot for Delsea Dr. N and New St.

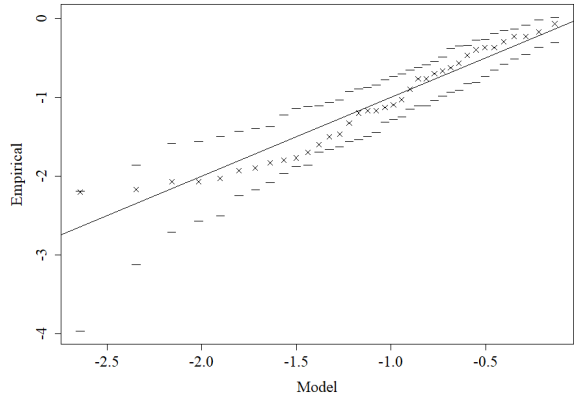

e) QQ plot for Delsea Dr. N and Donald Barger Blvd.

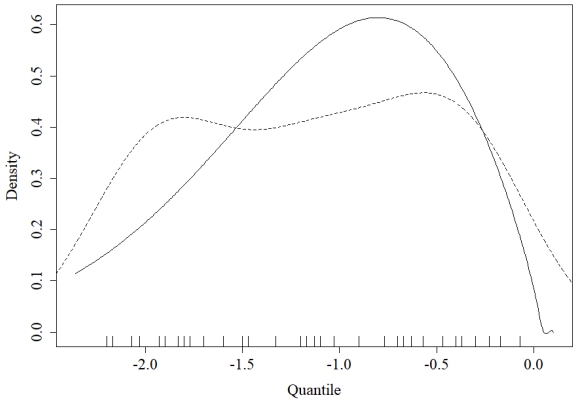

f) Density plot for Delsea Dr. N and Donald Barger Blvd.

Figure 11 Goodness of fit plots for PET for three locations

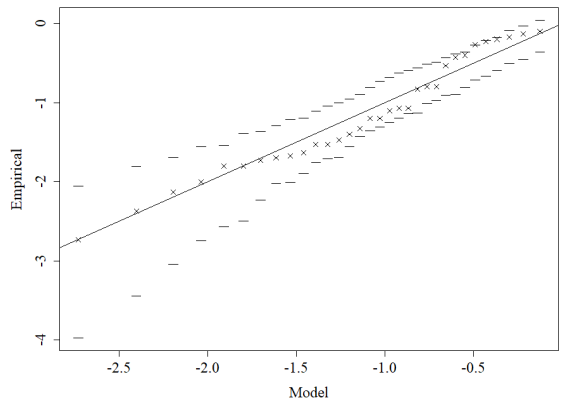

a) QQ plot for Delsea Dr. N and High St.

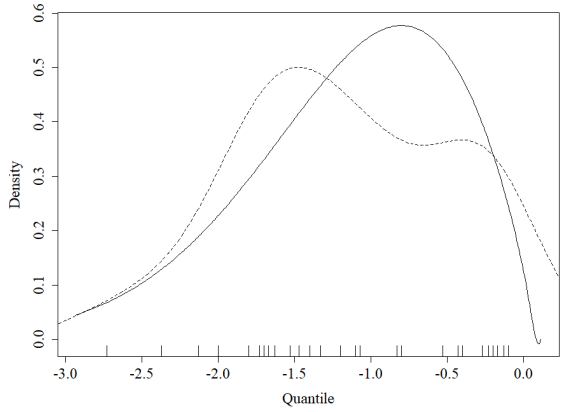

b) Density plot for Delsea Dr. N and High St.

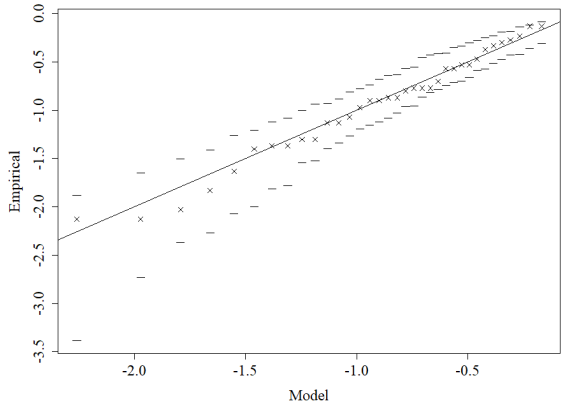

c) QQ plot for Delsea Dr. N and New St.

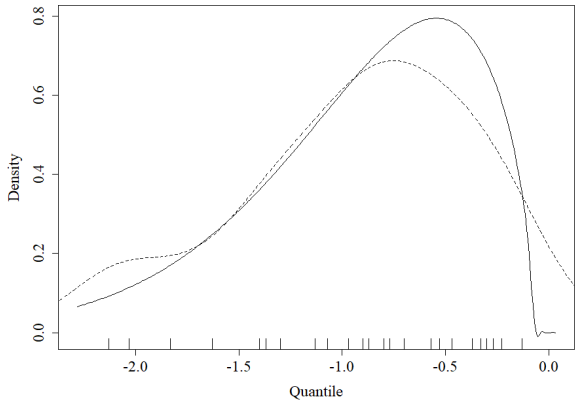

d) Density plot for Delsea Dr. N and New St.

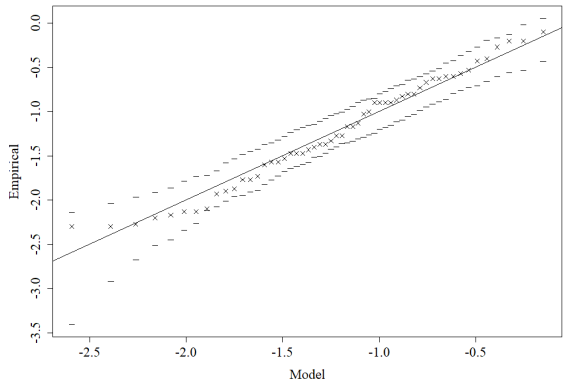

e) QQ plot for Delsea Dr. N and Donald Barger Blvd.

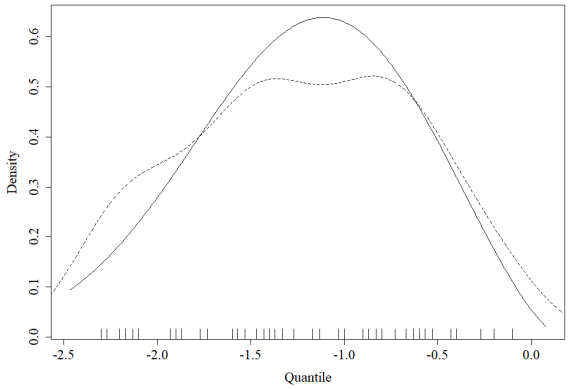

f) Density plot for Delsea Dr. N and Donald Barger Blvd.

Figure 12 Goodness of fit plots for TTC for three locations

Figure 13 illustrates the comparison between the estimated crashes by the models and the observed crashes. As shown in this figure, overall, the left-turn crashes by the models with PET and TTC were both estimated close to the observed left-turn crashes for all locations. Only the crashes using TTC for Delsea Dr. N and Donald Barger Blvd. intersection were estimated far from the observed

crashes. Moreover, the 95% C.I. of the estimated crashes using TTC were narrower than those of the estimated crashes using PET.

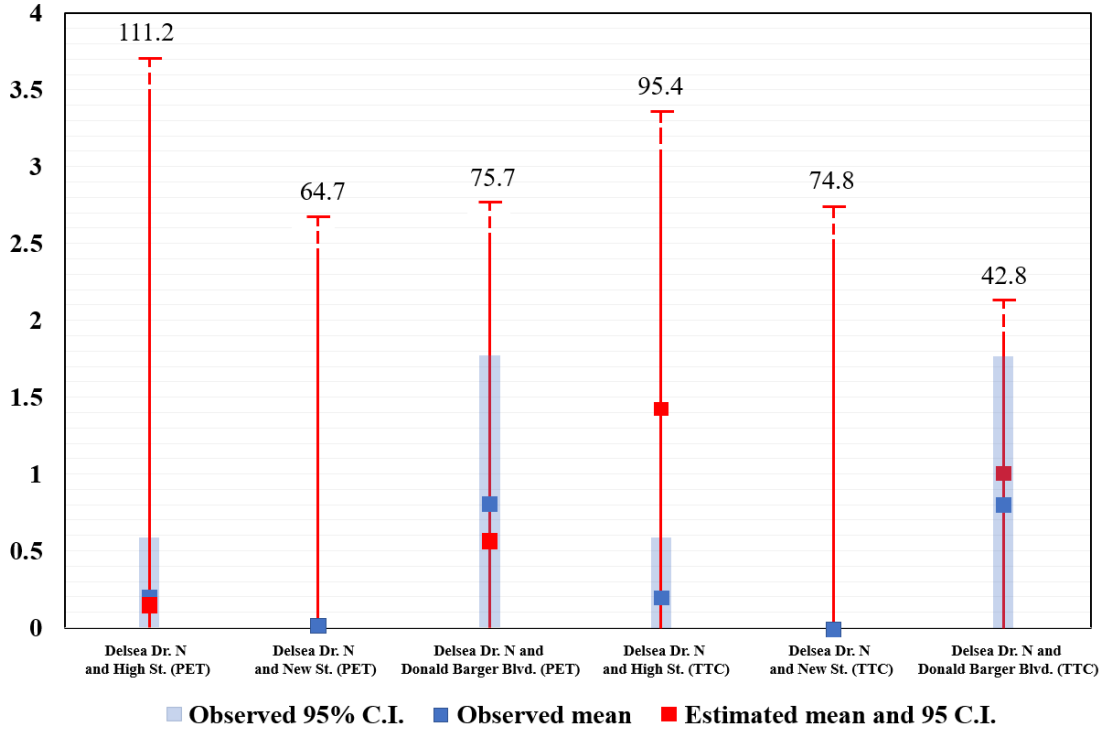

Figure 13 Comparison between the observed crashes and the estimated crashes

The final step for evaluating the safety of intersections is to rank the three locations (4-leg intersections) in terms of their safety. In this study, the intersections are ranked based on the value of their estimated EPDO crashes. The estimated number of left-turn crashes from GEV models with PET and TTC are total left-turn crashes. In order to get the severity distribution of the crashes, the New Jersey severity ratios were used. To calculate the severity ratios for New Jersey, as mentioned before in methodology section, the left-turn crashes for the entire state of New Jersey were obtained based on their severity levels from 2015 to 2019. Thereafter, severity ratios for different severity levels were calculated for each year separately. Finally, the ratios were averaged in order to get the yearly ratio for each severity for the entire study period. Table 10 tabulates the calculated ratios for different severity levels for the entire state of New Jersey.

As the next step, by having the severity distribution of the estimated crashes for each location, EPDO crashes can be calculated. It is noteworthy to remark that the EPDO index was computed using calibrated ratios according to the New Jersey crash costs provided by the 2016 Highway Safety Manual (Harmon et al., 2018). Table 11 provides the considered national and New Jersey comprehensive cost units used for EPDO computation in this study.

Table 10 Severity ratios for the entire New Jersey

Severity	Year					Average
	2015	2016	2017	2018	2019	
Fatal (K)	0.0027	0.0034	0.0027	0.0015	0.0035	**0.0027**
Suspected Serious Injury (A)	0.0059	0.0038	0.0062	0.0056	0.0148	**0.0072**
Suspected Minor Injury (B)	0.0629	0.0694	0.0683	0.0660	0.1338	**0.0801**
Possible Injury (C)	0.3119	0.3181	0.3237	0.3009	0.2300	**0.2969**
No Apparent Injury (O)	0.6166	0.6054	0.5992	0.6260	0.6179	**0.6130**

Table 11 Comprehensive Crash Cost in New Jersey

Severity	National Comprehensive Cost Units	NJ PCI Ratio	New Jersey Comprehensive Cost Units	Cost Ratio
K	$11,295,400	1.2501	$14,120,267	**949.19**
A	$655,000	1.2501	$818,809	**55.04**
B	$198,500	1.2501	$248,143	**16.68**
C	$125,600	1.2501	$157,011	**10.55**
O	$11,900	1.2501	$14,876	**1.00**

The calculated severity distribution of the estimated crashes, as well as the EPDO indices, are listed in Table 12. As can be seen in this table, the highest number of fatal crashes was estimated for Delsea Dr. N and High St. intersection for GEV model with TTC as the traffic conflict indicator. Moreover, the EPDO index for this location was computed as 11.6.

Table 12 Calculated severity distribution of the estimated crashes

Model	Location	Estimated Crashes	K	A	B	C	O	EPDO
GEV_PET	Delsea Dr. N and High St.	0.157	0.0004	0.0011	0.0126	0.0466	0.0963	1.3
	Delsea Dr. N and New St.	0	0.0000	0.0000	0.0000	0.0000	0.0000	0.0
	Delsea Dr. N and Donald Barger Blvd.	0.584	0.0016	0.0042	0.0468	0.1735	0.3582	4.7
GEV_TTC	Delsea Dr. N and High St.	1.429	0.0039	0.0103	0.1144	0.4242	0.8758	11.6
	Delsea Dr. N and New St.	0	0.0000	0.0000	0.0000	0.0000	0.0000	0.0
	Delsea Dr. N and Donald Barger Blvd.	1.01	0.0028	0.0073	0.0812	0.3010	0.6214	8.2

Subsequently, the EPDO indices were combined to get the final values for ranking the intersections. According to a previous study (Zheng and Sayed, 2019a), on average, the estimated crashes from GEV model using TTC were around nine times the estimated crashes from GEV model using PET. This relationship between the crashes estimated from TTC and PET models was implemented for weighting the EPDO indices for calculating the final combined EPDO scores. The combined EPDO score can be computed by summation of the weighted EPDOs from PET and TTC models for each location. Finally, the three intersections (4-leg intersections) were ranked based on their combined EPDO scores. The lower the value of the combined EPDO score, the safer the intersection would be. Table 13 presents the computed combined EPDO and the rankings for the three 4-leg intersections. As can be seen in this table, Delsea Dr. N and High St. intersection was found to be the un-safest intersection in terms of safety. Moreover, Delsea Dr. N and Donald Barger Blvd. intersection was ranked as the safest intersection among other locations.

Table 13 Calculated combined EPDO score and the ranking

Location	Combined EPDO Score	Ranking
Delsea Dr. N and High St.	103.3	**1**
Delsea Dr. N and Donald Barger Blvd.	77.1	**2**
Delsea Dr. N and New St.	0.0	**3**

CONCLUSION

The main intention of this study was to proactively evaluate the safety of intersections by using traffic conflicts and non-compliance behavior. To achieve this study's goal, an innovative artificial intelligence AI and a web-based Safety Analytics application were developed to detect, track, count, and recognize non-compliance behavior, such as vehicle redlight running and pedestrian jaywalking, identify road user conflicts, and conflict severity by SSM. In this study, SSMs, including PET and TTC, are used to identify future threats associated with the left-turning vehicles.

To evaluate the performance of the developed tools and assess the intersection safety, six intersections located in Glassboro, New Jersey, were selected. Afterward, nine hours of video data were recorded for each selected intersection. Overall, 54 hours of high-resolution video data consisting of more than 5.8 million frames were processed using the tool that integrated a real-time AI detection model - YOLO-v5 with a tracking framework based on the DeepSORT algorithm to extract trajectory data. Overall, the integrated model demonstrated an accuracy between 92 and 99 percent. The rate of non-compliance for the vehicles running a red light and pedestrian jaywalking was identified to understand the road-users behavior and gauge the intersection safety. The results showed that the intersection at New St and High St represented the highest rate of non-compliance for vehicles running a red light, i.e., 0.008 and 0.007 percent, respectively. Based on aggregated results for all the locations for the pedestrian non-compliance events, it can be observed that 1 in 4 pedestrians crossing the street is not entirely using a crosswalk to cross the street or is jaywalking.

For the conflict analysis, PET results showed that the intersection at Fishpond Rd had a higher percentage of the dangerous conflicts than other 3-leg intersection locations, i.e., 24.1 percent of the possible conflicts were less than 1.5 seconds. Furthermore, for the 4-leg intersections, the intersection at New St showed a higher percentage of the dangerous conflicts compared to other locations, i.e., 12.1 percent of the possible conflicts were less than 1.5 seconds. Similarly, the TTC results for the Fishpond Rd and New St showed a higher percentage of the dangerous conflicts than other 3-leg and 4-leg intersection locations, i.e., 27.0 and 14.6 percent of the potential conflicts were less than 1.5 seconds, respectively.

As the next step of this study, by using the extracted PETs and TTCs from the video data, GEV models with BM approach were developed to estimate the number of yearly left-turn crashes for the 4-leg intersections. Finally, by calculating the EPDO scores, the 4-leg intersections were ranked regarding their safety. According to the obtained results, the left-turn crashes from the developed GEV models were closely estimated to the observed crashes at the 4-leg intersections. The ranking results also revealed that Delsea Dr. N and West St. intersection is the unsafest location among all the 4-log intersections.

Despite the promising results achieved, there are some limitations in this study. Hence, some future researches are suggested by the authors to overcome the limitations and expand this work. As part

of future research, more video footage from different sources, such as 511.org, PTZ cameras, and other live streams, will be utilized to assess the model's robustness. Intersections with higher pedestrian volume will be considered to explore vehicle-to-pedestrian conflicts. Traffic signal phase data from Automated Traffic Signal Performance Measures (ATSPM) could be integrated with this tool to understand better traffic conflicts and non-compliance behaviors at each traffic cycle. Other safety indicators, like Deceleration Rate (DR), Gap Time (GT), and Proportion of Stopping Distance (PSD), could be calculated to assess the intersection safety extensively and help traffic safety practitioners to identify the future collision threats proactively. Moreover, only 4-leg intersections were used to develop the GEV models due to the low number of extracted PET and TTC data for 3-leg intersections. Hence, in the future, a longer duration of video data will be recorded for 3-leg intersections in order to include them in the analysis. In addition, more video data will be collected for more 4-leg intersections. Lastly, bivariate extreme value models will also be developed to compare the crash estimation results with the univariate models developed in this study.

REFERENCES

Alhajyaseen, W. K. (2015). The integration of conflict probability and severity for the safety assessment of intersections. *Arabian Journal for Science and Engineering*, *40*(2), 421-430.

Amundsen, F.H., and Hyden, C. (Eds.). (1977). Proceedings of the 1st Workshop on Traffic Conflicts, Oslo, Norway.

Arun, A., Haque, M. M., Bhaskar, A., Washington, S., & Sayed, T. (2021). A bivariate extreme value model for estimating crash frequency by severity using traffic conflicts. *Analytic Methods in Accident Research*, *32*, 100180.

Bewley, A., Ge, Z., Ott, L., Ramos, F., & Upcroft, B. (2016, September). Simple online and realtime tracking. In *2016 IEEE international conference on image processing (ICIP)* (pp. 3464-3468). IEEE.

Cai, Q., Abdel-Aty, M., Sun, Y., Lee, J., & Yuan, J. (2019). Applying a deep learning approach for transportation safety planning by using high-resolution transportation and land use data. *Transportation research part A: policy and practice*, *127*, 71-85.

Chen, P., Zeng, W., Yu, G., & Wang, Y. (2017). Surrogate safety analysis of pedestrian-vehicle conflict at intersections using unmanned aerial vehicle videos. *Journal of advanced transportation*, *2017*.

Cooper, D. F., & Ferguson, N. (1976). Traffic studies at T-Junctions. 2. A conflict simulation Record. *Traffic Engineering & Control*, *17*(Analytic).

El-Basyouny, K., & Sayed, T. (2013). Safety performance functions using traffic conflicts. *Safety science*, *51*(1), 160-164.

Essa, M., Sayed, T., 2018. Full Bayesian conflict-based models for real time safety evaluation of signalized intersections. Accident Analysis and Prevention 129, 367–381.

Federal Highway Administration (FHWA). (2021). Intersection Safety, U.S. Department of Transportation (USDOT). https://highways.dot.gov/research/research-programs/safety/intersection-safety

Federal Highway Administration (FHWA). (2022). About Intersection Safety, U.S. Department of Transportation (USDOT). https://safety.fhwa.dot.gov/intersection/about/

Fernandes, W., Naghettini, M., & Loschi, R. (2010). A Bayesian approach for estimating extreme flood probabilities with upper-bounded distribution functions. *Stochastic Environmental Research and Risk Assessment*, *24*(8), 1127-1143.

Formosa, N., Quddus, M., Ison, S., Abdel-Aty, M., & Yuan, J. (2020). Predicting real-time traffic conflicts using deep learning. *Accident Analysis & Prevention*, *136*, 105429.

Fu, T., Miranda-Moreno, L., & Saunier, N. (2016). Measuring crosswalk safety at nonsignalized crossings during nighttime based on surrogate measures of safety: Case study in Montreal, Canada. In *Transportation Research Board Annual Meeting Compendium of Papers*.

Fu, C., Sayed, T., & Zheng, L. (2020). Multivariate Bayesian hierarchical modeling of the non-stationary traffic conflict extremes for crash estimation. *Analytic methods in accident research*, *28*, 100135.

Harmon, T., Bahar, G. B., & Gross, F. B. (2018). *Crash costs for highway safety analysis* (No. FHWA-SA-17-071). United States. Federal Highway Administration. Office of Safety.

Hauer, E., & Garder, P. (1986). Research into the validity of the traffic conflicts technique. Accident Analysis & Prevention, 18(6), 471-481.

Hayward, J. C. (1972). Near miss determination through use of a scale of danger.

Hou, X., Wang, Y., & Chau, L. P. (2019, September). Vehicle tracking using deep sort with low confidence track filtering. In *2019 16th IEEE International Conference on Advanced Video and Signal Based Surveillance (AVSS)* (pp. 1-6). IEEE.

Jocher, G., Chaurasia, A., Stoken, A., Borovec, J., NanoCode012, Kwon, Y., TaoXie, Fang, J., Imyhxy, Michael, K., Lorna, V, A., Montes, D., Nadar, J., Laughing, Tkianai, yxNONG, Skalski, P., Wang, Z., … Minh, M. T. (2022, February 22). *Ultralytics/yolov5: V6.1 - tensorrt, tensorflow edge TPU and OpenVINO export and inference*. Zenodo. Retrieved July 2, 2022, from https://zenodo.org/record/6222936#.YsAltXbMKUk

Jonathan, P., & Ewans, K. (2013). Statistical modelling of extreme ocean environments for marine design: a review. *Ocean Engineering*, *62*, 91-109.

Laureshyn, A., de Goede, M., Saunier, N., & Fyhri, A. (2017). Cross-comparison of three surrogate safety methods to diagnose cyclist safety problems at intersections in Norway. *Accident Analysis & Prevention*, *105*, 11-20.

Lim, I. K., & Kweon, Y. J. (2013). Identifying High-Crash-Risk Intersections: Comparison of Traditional Methods with the Empirical Bayes–Safety Performance Function Method. *Transportation research record*, *2364*(1), 44-50.

Lin, T. Y., Maire, M., Belongie, S., Hays, J., Perona, P., Ramanan, D., ... & Zitnick, C. L. (2014, September). Microsoft coco: Common objects in context. In *European conference on computer vision* (pp. 740-755). Springer, Cham.

Lord, D. (1996). Analysis of pedestrian conflicts with left-turning traffic. *Transportation Research Record*, *1538*(1), 61-67.

Lord, D., & Mannering, F. (2010). The statistical analysis of crash-frequency data: A review and assessment of methodological alternatives. *Transportation research part A: policy and practice*, *44*(5), 291-305.

Manh, H., & Alaghband, G. (2018). Scene-lstm: A model for human trajectory prediction. *arXiv preprint arXiv:1808.04018*.

Mahmoud, N., Abdel-Aty, M., Cai, Q., & Yuan, J. (2021). Predicting cycle-level traffic movements at signalized intersections using machine learning models. *Transportation research part C: emerging technologies*, *124*, 102930.

Nadimi, N., Amiri, A. M., & Sadri, A. (2021). Introducing novel statistical-based method of screening and combining currently well-known surrogate safety measures. *Transportation Letters*, 1-11.

New Jersey State Department of State Police. (2019). Fatal Motor Vehicle Accident Comparative Data Report for the State of New Jersey, 2019

Rocco, M. (2014). Extreme value theory in finance: A survey. *Journal of Economic Surveys*, *28*(1), 82-108.

Redmon, J., Divvala, S., Girshick, R., & Farhadi, A. (2016). You only look once: Unified, real-time object detection. In *Proceedings of the IEEE conference on computer vision and pattern recognition* (pp. 779-788).

Redmon, J., & Farhadi, A. (2018). Yolov3: An incremental improvement. *arXiv preprint arXiv:1804.02767*.

Saunier, N., Sayed, T., & Ismail, K. (2010). Large-scale automated analysis of vehicle interactions and collisions. *Transportation Research Record*, *2147*(1), 42-50.

Sayed, T., & Zein, S. (1999). Traffic conflict standards for intersections. *Transportation Planning and Technology*, *22*(4), 309-323.

Sayed, T., Zaki, M. H., & Autey, J. (2013). Automated safety diagnosis of vehicle–bicycle interactions using computer vision analysis. *Safety science*, *59*, 163-172.

Scholl, L., Elagaty, M., Ledezma-Navarro, B., Zamora, E., & Miranda-Moreno, L. (2019). A surrogate video-based safety methodology for diagnosis and evaluation of low-cost pedestrian-safety countermeasures: the case of cochabamba, bolivia. *Sustainability*, *11*(17), 4737.

Simonnet, D., Velastin, S. A., Turkbeyler, E., & Orwell, J. (2012). Backgroundless detection of pedestrians in cluttered conditions based on monocular images: a review. *IET Computer Vision*, *6*(6), 540-550.

Tarko, A., Davis, G., Saunier, N., Sayed, T., & Washington, S. (2009). Surrogate measures of safety. White paper. *Transportation Research Board, Washington, DC*.

Torrielli, A., Repetto, M. P., & Solari, G. (2013). Extreme wind speeds from long-term synthetic records. *Journal of Wind Engineering and Industrial Aerodynamics*, *115*, 22-38.

Wang, C., Xu, C., Xia, J., Qian, Z., & Lu, L. (2018). A combined use of microscopic traffic simulation and extreme value methods for traffic safety evaluation. *Transportation Research Part C: Emerging Technologies*, *90*, 281-291.

Wang, C., Xu, C., & Dai, Y. (2019). A crash prediction method based on bivariate extreme value theory and video-based vehicle trajectory data. *Accident Analysis & Prevention*, *123*, 365-373.

Wang, H., Tong, X., & Lu, F. (2020, November). Deep learning based target detection algorithm for motion capture applications. In *Journal of Physics: Conference Series* (Vol. 1682, No. 1, p. 012032). IOP Publishing.

Wang, Y., Zhang, D., Liu, Y., Dai, B., & Lee, L. H. (2019). Enhancing transportation systems via deep learning: A survey. *Transportation research part C: emerging technologies*, *99*, 144-163.

Xie, K., Li, C., Ozbay, K., Dobler, G., Yang, H., Chiang, A. T., & Ghandehari, M. (2016, November). Development of a comprehensive framework for video-based safety assessment. In *2016 IEEE 19th International Conference on Intelligent Transportation Systems (ITSC)* (pp. 2638-2643). IEEE.

Xie, K., Ozbay, K., Yang, H., & Li, C. (2019). Mining automatically extracted vehicle trajectory data for proactive safety analytics. *Transportation research part C: emerging technologies*, *106*, 61-72.

Yang, D., Xie, K., Ozbay, K., & Yang, H. (2021). Fusing crash data and surrogate safety measures for safety assessment: Development of a structural equation model with conditional autoregressive spatial effect and random parameters. *Accident Analysis & Prevention*, *152*, 105971.

Zangenehpour, S., Miranda-Moreno, L. F., & Saunier, N. (2015). Automated classification based on video data at intersections with heavy pedestrian and bicycle traffic: Methodology and application. *Transportation research part C: emerging technologies*, *56*, 161-176.

Zangenehpour, S., Strauss, J., Miranda-Moreno, L. F., & Saunier, N. (2016). Are signalized intersections with cycle tracks safer? A case–control study based on automated surrogate safety analysis using video data. *Accident Analysis & Prevention*, *86*, 161-172.

Zhang, S., Abdel-Aty, M., Wu, Y., & Zheng, O. (2020). Modeling pedestrians' near-accident events at signalized intersections using gated recurrent unit (GRU). *Accident Analysis & Prevention*, *148*, 105844.

Zheng, L., & Sayed, T. (2019a). From univariate to bivariate extreme value models: approaches to integrate traffic conflict indicators for crash estimation. *Transportation research part C: emerging technologies*, *103*, 211-225.

Zheng, L., & Sayed, T. (2019b). Bayesian hierarchical modeling of traffic conflict extremes for crash estimation: a non-stationary peak over threshold approach. *Analytic methods in accident research*, *24*, 100106.

Zheng, L., & Sayed, T. (2020). A bivariate Bayesian hierarchical extreme value model for traffic conflict-based crash estimation. *Analytic methods in accident research*, *25*, 100111.

Zheng, L., Ismail, K., & Meng, X. (2014a). Freeway safety estimation using extreme value theory approaches: A comparative study. *Accident Analysis & Prevention*, *62*, 32-41.

Zheng, L., Ismail, K., & Meng, X. (2014b). Traffic conflict techniques for road safety analysis: open questions and some insights. *Canadian journal of civil engineering*, *41*(7), 633-641.

Zheng, L., Ismail, K., Sayed, T., & Fatema, T. (2018). Bivariate extreme value modeling for road safety estimation. *Accident Analysis & Prevention*, *120*, 83-91.

Zheng, L., Sayed, T., & Essa, M. (2019a). Validating the bivariate extreme value modeling approach for road safety estimation with different traffic conflict indicators. *Accident Analysis & Prevention*, *123*, 314-323.

Zheng, L., Sayed, T., & Essa, M. (2019b). Bayesian hierarchical modeling of the non-stationary traffic conflict extremes for crash estimation. *Analytic methods in accident research*, *23*, 100100.